ABSTRACT

Title of dissertation:	Rapid kinetics study of the nuclease activity of RecBCD enzyme from *Escherichia coli*
	Archana Ghatak, Doctor of Philosophy, 2006
Dissertation directed by:	Prof. Douglas A. Julin Department of Chemistry and Biochemistry

RecBCD enzyme from *Escherichia coli* is involved in homologous recombination and repair of bacterial DNA, and in defending the cell against foreign DNA. This enzyme has multiple functions – it is an ATP-stimulated ssDNA endonuclease, an ATP-dependent ssDNA and dsDNA exonuclease and a DNA helicase. Here we investigated the kinetics of the exonuclease reaction of RecBCD.

We purified the enzyme from *E. coli* by using conventional adsorption chromatography. The exonuclease function was studied using a rapid quench-flow (RQF) instrument designed by Kintek Corporation. Short single-stranded DNA oligomers were labeled with ^{32}P ATP at the 5′ end and used as substrates.

Our goal was to study the reaction products as the enzyme travels along the DNA. From earlier studies it is known that the enzyme binds at the end of a double-stranded DNA, unwinds and cleaves the DNA as it moves. This enzymatic movement can be very fast, in the range of 500−1000 base-pairs per second. We carried out exonuclease reactions using the RQF instrument for time periods ranging from 10 msec to 2 sec. The time courses of appearance and change of the amounts of the labeled products displayed in sequencing gels were analyzed using a Phosphorimager

and associated software. A kinetic model for the enzyme was derived by analyzing the time course data with Kinteksim, a simulation program.

We were able to identify the reaction products of the single turnover exonuclease reactions. For the first time we were able to show that the enzyme does not cleave a DNA substrate at every nucleotide even in conditions where it acted as a potent exonuclease. Rather, our results suggested that the enzyme moves along the DNA and cleaves in steps of 2-4 nucleotides. The enzyme concentration used in our study was almost 10 times more than the DNA concentration in order to make sure that all DNA molecules were bound to enzyme. Still not all DNA molecules participated in the nuclease reaction in the single turnover reaction time period, suggesting that some of the DNA enzyme complexes were inactive with respect to the nuclease activity.

The rate of translocation of the enzyme along the DNA varied with the change of concentration of ATP in the reaction. However, the products were the same at several ATP concentrations. Our results indicate the presence of at least two ATP dependent steps after the reaction is started and before the first nuclease product appears. These steps are proposed to represent the translocation of the DNA end from the binding site to the nuclease active site. Also, our results suggest that the rate of translocation at each ATP concentration is similar to the unwinding rate of a double stranded DNA at the same ATP concentration [determined by Lucius, A. L. & Lohman, T. M. (2004) *J Mol Biol* 339, 751-771.]

Rapid kinetics study of the nuclease activity of RecBCD enzyme from *Escherichia coli*

by

Archana Ghatak

Dissertation submitted to the Faculty of the Graduate School of the
University of Maryland, College Park, in partial fulfillment
of the requirements for the degree of
Doctor of Philosophy
2006

Advisory Committee:

Professor Douglas A. Julin, Chair
Professor Dorothy Beckett
Professor Jason Kahn
Professor Zvi Kelman
Professor Jeffrey DeStefano

DEDICATION

To Baba and Ma,

with love and gratitude

ACKNOWLEDGEMENTS

The years of my Ph.D. research and days of my course work at the Department of Chemistry and Biochemistry, University of Maryland, have been the most fruitful time of my life so far, which has been influenced in so many ways by so many people. I take this opportunity to acknowledge them all.

Firstly I convey my heartfelt thanks to my supervisor Professor Douglas Julin for guiding and helping me to carry out the research work pertaining to this thesis. I am deeply grateful to him for introducing and giving me necessary exposure in the world of RecBCD.

I express my gratitude towards Professor Dorothy Beckett (U. Md.), Professor Jason Kahn (U. Md.) and others with whom I had illuminating discussions on various problem of my work at several occasions. I convey my reverence to my teachers of my course work at University of Maryland during the first few years.

I would like to thank all members of the Department of Chemistry and Biochemistry for creating a congenial atmosphere which made working here most enjoyable. Particularly, I thank Mathew, Steven, William and others. Besides, I would like to acknowledge the help provided by the staff at business office. I also thank my friends Gunjan, Vanaja, Sripriya and others for the company they provided and making my stay in USA most enjoyable.

Last, but not the least, I am greatly indebted to my parents, my brother and my husband who remain a perpetual source of encouragement and inspiration through the difficulties during all these years of my Ph.D.

Table of Contents

List of Tables

List of Figures

List of Abbreviations

DTT	Dithiothreitol
EDTA	Ethylenediaminetetraacetic acid
FRET	Fluoroscence resonance energy transfer
IPTG	Isopropyl-β-thiogalactopyranoside
RQF	Rapid quench-flow
SDS-PAGE	Sodium dodecyl sulfate – polyacrylamide gel electrophoresis
SSB	Single strand binding protein
TCA	Trichloroacetic acid
TLC	Thin layer chromatography

INTRODUCTION:

An unrepaired DNA break is lethal for any cell [Lange (1975)]. Double stranded DNA (dsDNA) breaks can be produced by ionizing radiation, such as γ rays [Resnick et al. (1976)]. They can also be formed during normal DNA replication when the DNA polymerase encounters a nick on a DNA template [Kowalczykowski (2000)]. Single stranded DNA (ssDNA) gaps can arise from the repair of DNA damage, or from blocked DNA replication. The enzymes involved in homologous recombination act at these double stranded DNA breaks and single stranded DNA gaps to carry out the events that result in gene recombination, as well as the repair of the damaged replication arms and the resumption of DNA replication. Thus recombination is an important component of DNA replication and repair. The recombination related repair process (Fig. 1) consists of four steps: (1) initiation (processing), (2) homologous pairing and DNA strand exchange, (3) DNA hetero-duplex extension (branch migration) and (4) resolution [Kowalczykowski (2000)].

There are at least 25 different proteins that are involved in different types of homologous recombination in *E. coli*. Some examples are RecA, RecBCD, RecF, RecG, RecJ, RecN, RecO, RecQ, RecR, RuvAB, RuvC, PriA and SSB proteins, DNA polymerases, DNA topoisomerases and DNA ligase, and the regulatory DNA sequence, *Chi* (χ) [Kowalczykowski (2000)]. Each of these proteins, alone or in combination with other proteins, takes part in different steps of recombination.

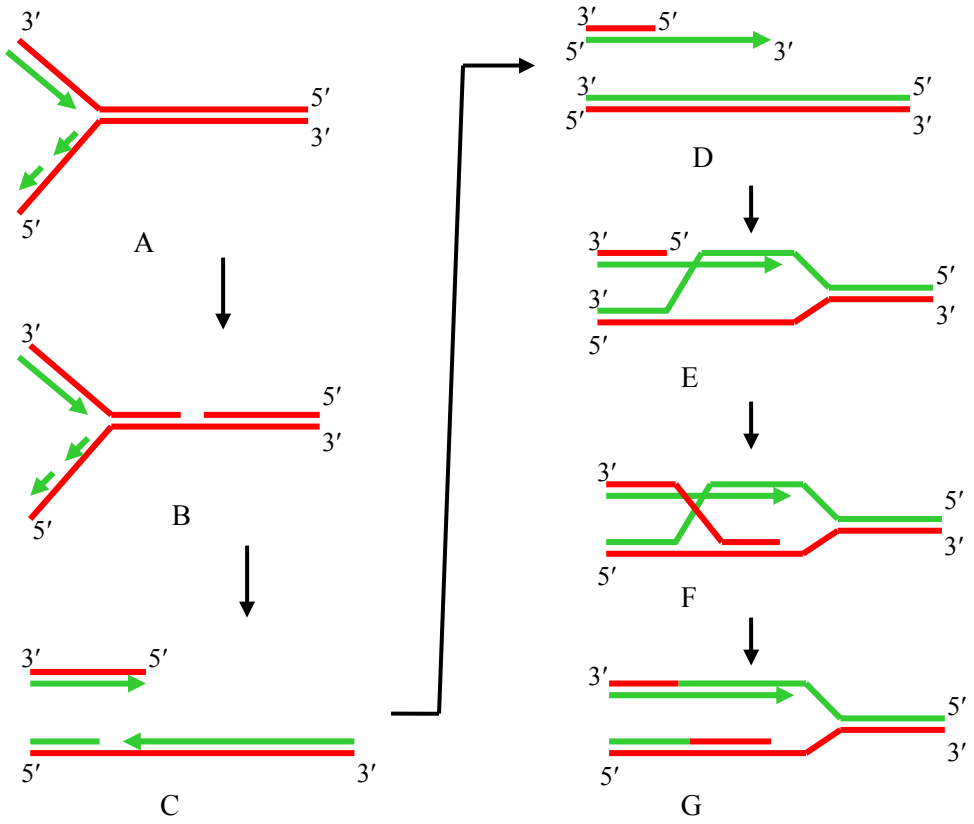

Fig. 1: Recombinational repair of double stranded breaks during replication.

A. Replication fork in a double stranded DNA with leading and lagging strands.

B. Single stranded gap in the replicating DNA.

C. Double-stranded break when replication fork reaches a single-stranded gap.

D. Creation of a 3' end single strand by a recombination machinery (e.g. RecBCD), initiating recombinational repair.

E. Strand invasion and homologous pairing.

F. Branch migration.

G. Holliday junction resolution and restoration of replication fork.

RecBCD and RecA proteins take part in most of the recombination events and in the double stranded break repair in wild type *E. coli*. RecBCD can process a DNA at the initial stage of recombination (steps C → D, Fig. 1, steps A-C, Fig. 2) and it loads RecA on a 3' DNA single strand (step D, Fig. 2). RecA protein, bound to a DNA strand, searches for a sequence which is homologous to that of the strand it is bound to (step E, Fig. 2). This causes homologous pairing (step E, Fig. 1) and DNA strand exchange.

DNA heteroduplex extension (step F, Fig. 1) is carried out by the RuvAB complex. RuvAB is a helicase, and it causes branch migration of the cross-over point. RuvC is a Holliday-junction specific endonuclease. It acts in complex with RuvAB. RuvC completes the recombination process by cleaving Holliday junctions [West (1997)]. RecG is another helicase which is known to be involved in the formation of a Holliday junction from a blocked replication fork by a process called replication fork regression [McGlynn and Lloyd (2001)].

Another pathway for initiation of recombination is the RecF pathway. It acts by a mechanism which is different from that of the RecBCD pathway. This pathway involves several different enzymes to process the DNA. RecQ helicase unwinds the DNA. RecJ is a 5'-3' single stranded DNA exonuclease. It makes a 3' terminated DNA end that is coated with single strand binding protein (SSB). RecF, RecO and RecR function as a complex and they replace SSB to finally create a DNA strand coated with RecA [Amundsen and Smith (2003)].

Here we will discuss in detail the initiation of recombination by the RecBCD enzyme, its multiple enzymatic functions, processing of DNA strands, and regulation.

Initiation of recombination: RecBCD

The RecBCD enzyme from *Escherichia coli* is a multifunctional enzyme that plays an important role in homologous genetic recombination, repair of double stranded DNA breaks, resistance to UV irradiation and chemical DNA damaging agents, and degradation of foreign DNA. It has a number of different enzymatic activities, including ATP-dependent exonuclease, ATP-stimulated endonuclease, DNA dependent ATPase, and DNA helicase activities [Kowalczykowski et al. (1994), Smith (1990), Muskavitch and Linn (1981)]. The enzyme consists of three protein subunits encoded by the *recB*, *recC*, and *recD* genes. The molecular masses of the RecB, RecC, and RecD subunits are 134, 129, and 67 kDa, respectively (Finch et al, 1986). RecBCD performs two important functions in the *E. coli* cell. It can degrade any foreign linear dsDNA, such as the genomes of bacteriophages λ and T_4, unless they are protected by some mechanism. For example, RecBCD inhibits rolling circle DNA replication in phage λ [Enquist and Skalka (1973), Skalka (1977)]. The product of the gene 2 of phage T4, or Gam protein from phage λ are needed for protection of phage T4 or λ, respectively, from RecBCD [Poteete et al. (1988), Behme et al. (1976), Oliver and Goldberg (1977)]. RecBCD also helps *E. coli* to recover from double stranded breaks in its chromosome during genomic replication [Kuzminov (1995)] and to maintain its viability [Kuzminov and Stahl (1999)].

RecBCD takes part in the initial processing of the double stranded (ds) DNA (Fig. 2). The enzyme binds strongly at the end of a dsDNA (Fig. 2, step A). Such a dsDNA end could arise due to a double stranded DNA break. Gabbidon et al. (1998) studied RecBCD-DNA binding by a nitrocellulose filter binding assay. The enzyme binding to the end of a dsDNA containing a small 3' overhang showed a K_d of 4.9 nM in the absence of ATP and in the presence of 0.2 M NaCl.

In the presence of ATP the enzyme then starts unwinding the DNA by its helicase activity. At the same time it starts cleaving the 3' end strand by its exonuclease activity (Fig. 2, step B). There is an 8 nucleotide sequence, called *Chi* sequence (5'-GCTGGTGG-3'), which occurs very frequently in the *E. coli* genome. There is one *Chi* site per 4-5 kb of the *E. coli* genome, which is much more than the expected random occurrence of an eight nucleotide sequence [Kuzminov et al. (1994)]. When the moving RecBCD molecule meets the *Chi* sequence on the 3' strand, it stops cleaving the strand. Instead it starts cleaving the 5' strand in the 5'-3' direction (Fig.2, step C).

Anderson and Kowalczykowski (1997) defined the different regions of the two strands of a *Chi*-containing double stranded DNA with respect to the *Chi* sequence. They defined the region between the *Chi* sequence and the end of the DNA where the enzyme starts unwinding the DNA as the upstream region, and the region between the *Chi* sequence and the opposite end of the DNA as the downstream region. Also they called the DNA containing the *Chi* sequence as the top strand and the opposite strand as the bottom strand.

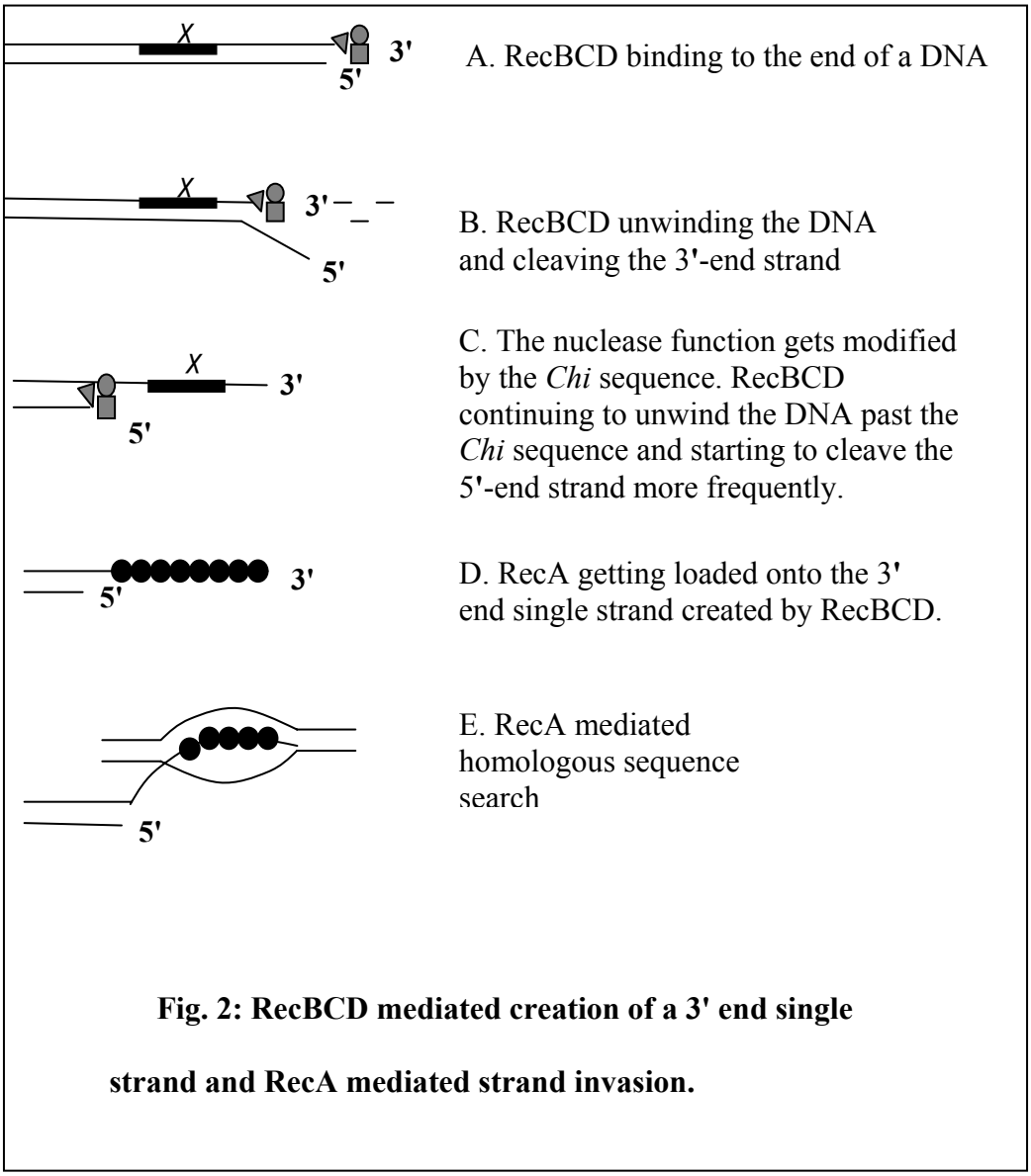

Fig. 2: RecBCD mediated creation of a 3' end single strand and RecA mediated strand invasion.

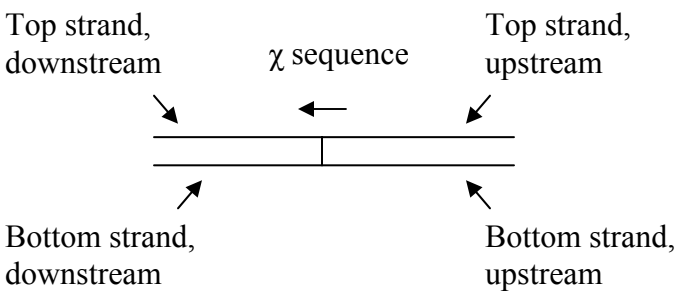

Fig. 3: **Different regions of the two strands of a *Chi* containing double stranded DNA with respect to the *Chi* sequence.**

The attenuation of the 3'-5' exonuclease activity and the start of the 5'-3' exonuclease activity on encountering the *Chi* sequence is known as the polarity switch of the exonuclease activity of RecBCD. This was first noticed by Dixon and Kowalczykowski (1995). They allowed RecBCD to react with a *Chi*-containing DNA. They found that two *Chi*-specific strands were formed, one corresponding to the top strand downstream region and the other corresponding to the bottom strand upstream region.

Anderson and Kowalczykowsky (1997) confirmed that polarity switch really occurs in the presence of *Chi* and eliminated the possibility that the bottom strand *Chi*-specific fragment is formed as a result of a cut on the bottom strand made by a

second RecBCD molecule entering through the 5' end of the top strand (or 3' end of the bottom strand). They blocked the entry of the enzyme through one end of the DNA by creating a single stranded overhang, more than 25nt long. The enzyme could enter only through the other end and it could meet the *Chi* sequence only in the proper orientation (i.e. from the 3' direction). In this case also they saw the *Chi*-specific fragment from the bottom strand, as expected when the enzyme is free to enter through both ends. This confirmed the hypothesis that after interaction within the *Chi* site, the enzyme switches strands and starts degrading the bottom strand in the 5'-3' direction.

Although there is a change in the nuclease activity on encountering the *Chi* sequence, the helicase activity remains unaffected. The enzyme keeps on unwinding the DNA, moving along it and cleaving the 5' end DNA, until it finally dissociates from the DNA. Finally what is left is a long single stranded 3' end DNA at the end of double stranded DNA [Myers and Stahl (1994)]. RecA protein is loaded on this 3' end single stranded DNA (Fig. 2, stepD). DNA bound RecA begins homologous sequence search (Fig. 2, stepE). It is then followed by homologous pairing and DNA strand exchange [Arnold and Kowalczykowski (2000)].

It has been speculated by Wang et al. (2000), and Singleton et al. (2004) that the key to the regulation of the enzyme by *Chi* lies in the sequence specific interaction of the *Chi* sequence of the bound DNA and some region of the RecC subunit. They proposed that when the *Chi* sequence meets the specific peptide sequence in RecC it gets bound to it tightly and the 3' end cannot move any further towards the nuclease site. Since the nuclease site cannot access the 3' strand, it cleaves the 5' strand more

frequently. The helicase domain of RecB cannot recognize the *Chi* sequence and its activity remains unaffected when the *Chi* sequence is bound to the RecC subunit. So, the enzyme keeps unwinding the DNA and the part of the DNA between the *Chi* sequence and the helicase active site of the enzyme loops out.

Studies with RecBCD enzyme carrying mutations in the RecC subunit have helped to identify the specific region in the RecC subunit which is important for the *Chi* recognition [Schultz et al. (1983), Arnold et al. (2000)]. This region (residues 647-663) is a part of the channel of RecC, through which the 3' strand passes on its way to the nuclease site. This particular region is 20-25 Å away from the nuclease site [Singleton et al. (2004)]. When the Chi sequence is bound to this region, the nuclease site can make the last cleavage on the 3' strand, 4-6 nucleotides upstream of the Chi sequence, which is the shortest distance between the RecC Chi recognition site and the nuclease domain.

RecBCD in defense mechanism:

RecBCD can also bind at the end of a DNA which is foreign to *E. coli* and can start unwinding in the presence of ATP. But the chance that *Chi* sequence will be present in such a DNA is low. In that case RecBCD keeps unwinding the DNA and cleaving the 3' end. Enzyme molecules can bind at each end of such DNA, and each molecule cleaves the strand which runs 3' to 5' in the direction of the translocation of the enzyme. At the end both strands are destroyed. Thus the enzyme can be a potential role player in defense mechanism of the bacteria.

The nuclease active site of RecBCD:

Yu et al. (1998) identified the nuclease active site in the subunit B of RecBCD. The RecB subunit consists of a 100KDa N-terminal domain and a 30KDa C-terminal domain which are connected to each other by a linker region. This linker region is susceptible to proteolytic cleavage. By sequence comparison, Yu et al. found a motif in the C-terminal part of RecB, Ile-Asp-Xaa_{12}-Asp(*)-Tyr-Lys, within residues 1066-1082. This motif is conserved among RecB homologs in different bacteria and it is similar to a motif (Pro-Asp-$Xaa_{15\text{-}19}$-Asp-Xaa-Lys), forming a part of the active sites of some endonucleases [Kim et al. (1990), Newman et al. (1994), Grasby and Connolly (1992)]. Yu et al. made a point mutation that changed the highly conserved Asp1080 (indicated by the *) of RecB to Ala. This mutation abolished all nuclease activities of the enzyme. Earlier the N-terminal part of the enzyme was found to possess the ATP binding and hydrolysis activity. These properties remained unaffected by the mutation. So the mutant enzyme retained the ability to unwind a double-helix. This experiment clearly showed that the 30 kDa C-terminal domain of RecB contained all the nuclease activity of RecBCD. In 2000, Wang et al. made mutations at two other conserved amino acids in the RecB C-terminal domain. These two mutant proteins ($RecB^{D1067A}CD$ and $RecB^{K1082Q}CD$) also had inactivated nuclease activities.

The nuclease domain of the RecB protein has been found to be a member of the RecB family in Superfamily I of enzymes known as ‘endonuclease fold containing nucleases’. In many cases this domain has been found to be in combination with a

superfamily I helicase domain. Therefore it is suggested that this domain generally functions in a close association with DNA unwinding [Aravind et al. (2000)].

ATPase activity of RecBCD and its relation to its helicase and nuclease functions:

The RecBCD enzyme is an ATP-dependent nuclease and helicase [Kowalczykowski et al.(1994), Smith (1990), Muskavitch and Linn (1981)]. It uses ATP hydrolysis for rapid and processive unwinding of linear dsDNA and it cleaves the DNA, while unwinding it. RecBCD carries out this degradation by endonucleolytic reactions, forming short single stranded oligomers of different sizes, but not mononucleotides [Goldmark and Linn (1972), Chen et al. (1998)]. The enzyme displays highest nuclease activities under conditions where magnesium ion is present in excess over the ATP [Eggleston (1993)].

Julin and Lehman (1987) showed that both RecB and RecD bind ATP in the RecBCD holoenzyme. They covalently photolabeled the RecB and the RecD subunits with the ATP photoaffinity analogue [α-^{32}P]8-azido-ATP. ATP inhibited the photo-labeling of this analogue to the protein. It was found that RecBCD could hydrolyze this molecule and the hydrolysis supported the exonuclease activity of the enzyme. On tryptic digestion of the photolabeled holoenzyme, the label was found to be bound to mainly two peptides, one from the RecB subunit and the other from the RecD subunit. Thus, either or both of the RecB and RecD subunits could be responsible for the stimulation by ATP, since both proteins bind ATP and both proteins alone have

low level of DNA-dependent ATP hydrolysis activity [Masterson et al. (1992), Chen et al. (1997)].

Chen et al. (1998) carried out ATP hydrolysis studies with the subunits of RecBCD. γ-^{32}P-ATP was used as the substrate in this reaction. RecBCD hydrolyses this substrate to form ^{32}P-P_i, which could be separated from the substrate by thin layer chromatography, and quantitated by phosphor-imaging. They found that both RecB and RecD had greater ATPase activity when they were assembled in the RecBCD holo enzyme than when they were alone.

Chen et al. (1998) also did nuclease studies with RecBCD containing mutations in the ATP binding sites of RecB and RecD. Nuclease reactions were done with 25nt single stranded DNA substrates, which were labeled at the 5' end, using γ-^{32}P ATP, and at the 3' end, with α-^{32}P ddATP. The labeled DNA was mixed with the enzyme in a reaction mixture containing Mg^{++} and ATP. Small aliquots were removed, quenched, and analyzed by non-denaturing polyacrylamide gel electrophoresis. The radioactivity on the dried gel was analyzed by phosphorimaging. Their studies showed that RecBCD could cleave short single stranded oligomers in the absence of ATP mostly near the 5' end. This cleavage was almost 3000 fold slower than when ATP was added.

Chen et al. also used RecBCD enzymes containing mutations in the ATP binding sites of RecB and RecD. RecB-K29Q-CD enzyme (referred to as RecB*CD) contained a mutation in the ATP binding site of RecB; whereas, RecBCD-K177Q enzyme (referred to as RecBCD*) contained the mutation in the ATP binding site of RecD. Both the mutants showed nuclease activity on single stranded DNA, but the

nuclease activities were qualitatively different. RecB*CD made short 2-3 nucleotide oligomers by nuclease activities on 5' labeled DNA, which was an indication that RecB*CD cleaved the DNA near the 5' end. When 3' labeled DNA was used, the nuclease cleavage products were larger, indicating that the cleavage occurred away from the 3' end. Unlike RecB*CD, RecBCD* was found to cleave the DNA mainly near the 3' end and away from the 5' end. This shows that ATP binding to RecB facilitates nuclease activity which starts near the 3' end, while ATP binding to RecD is necessary for nuclease activity which starts near the 5' end.

The nuclease activity of the wild type RecBCD enzyme was similar to that of RecBCD*, in terms of end specificity. It formed similar nuclease products as RecBCD* , with 5' and 3' end labeled oligomers. From quantitative analysis of the bands, it was found that the amount of nucleolytic cleavage near the 5' end done by RecB*CD was much less than the cleavage near the 3' end done by RecBCD* or RecBCD.

Dillingham et al. (2003) did helicase assays with RecB, RecD and RecBCD. They used DNA oligomers with 5' or 3' single stranded overhangs as substrates. Their studies showed that RecD translocates in the 5'-3' direction and thus acts as a 5'-3' helicase motor. The translocation polarity of the RecB subunit is the opposite and it acts as a 3'-5' helicase. This result is consistent with the end specificity observed by Chen et al. (1998) as described above. When the enzyme binds to any dsDNA end, RecB binds to the 3' end while RecD binds to the 5' end. According to the model proposed by Dillingham et al. (2003), the unwinding and translocation activity of

RecBCD consists of two motor activities of opposite polarity. Together these subunits make the enzyme move faster with high processivity on a DNA substrate.

Pre-steady state kinetic study of the helicase function:

Lucius et al. (2004) studied pre-steady state kinetics of DNA unwinding by RecBCD helicase. They used DNA hairpins, labeled with fluorescent and radioactive labels, as substrates. The hairpin had a nick in the 5' strand. The enzyme first binds at the blunt end and starts unwinding it with the addition of ATP. Eventually, it reaches the nick and the portion of the 5' strand between the blunt end and the nick is released in the solution. In their study with radioactively labeled oligomers [Lucius et al. (2002)], they analyzed their product by polyacrylamide gel electrophoresis and then quantitated with phosphor-imaging. They also carried out similar studies (2004a, 2004b) with oligomers with fluorescent labels in a stopped flow instrument. They used DNA substrates labeled with Cy3 (donor) and Cy5 fluorophores (acceptor). Before the unwinding reaction started, both the fluorophores were in close proximity, across a single stranded nick. As a result, they could undergo fluorescence resonance energy transfer (FRET). Unwinding of the DNA caused release of one part of a DNA strand as described above, and the fluorophores became separated from each other. This gave rise to a fluorescent signal. They worked with oligomers of different lengths by including the nick at different positions of the 5' strand. The unwinding time courses are biphasic, with a fast phase following a lag phase and a much slower second phase. The length of the lag phase is related to the length of the released oligomer. Almost 70% of the DNA molecules are unwound during the fast phase. The

slower second phase was proposed to arise because some DNA molecules are bound to the enzyme in a non-productive mode, which undergoes a slow isomerization with the productive mode.

Lucius et al. analyzed the data obtained from the time course by non linear least squares analysis. They came up with several mechanisms, derived the kinetic equations corresponding to those mechanisms, and then simulated graphs using those equations. They checked how well these graphs fit to the data and whether the parameters were meaningful or not. Finally they had one mechanism (Fig. 4) that explained fully the kinetic steps that may occur during the unwinding reaction. They also used the same mechanism to study helicase activity of RecBCD at different ATP concentrations.

Fig. 4 shows the reaction scheme that describes the mechanism proposed by Lucius et al. (2002, 2004). In this mechanism, the unwinding of a double helix consists of a number of similar steps called unwinding steps, with rate constant k_U. In each step three to four base pairs get unwound. The DNA was pre-incubated with the enzyme before starting the experiment. The enzyme was added in excess, so, presumably, all DNA molecules had enzyme bound to their ends. They assumed that some of the DNA-enzyme complex remains bound in a non-productive state [$(R\bullet D)_{NP}$], which is in equilibrium with the productive state [$(R\bullet D)_L$]. $I_{(L-m)}$, $I_{(L-2m)}$, etc, are the partially unwound DNA intermediates, while, ssDNA is the fully unwound final product. They also determined the number of steps required to unwind the double helix of length L fully (‘n’), and the step size ‘m’ (bp unwound per step = L/n).

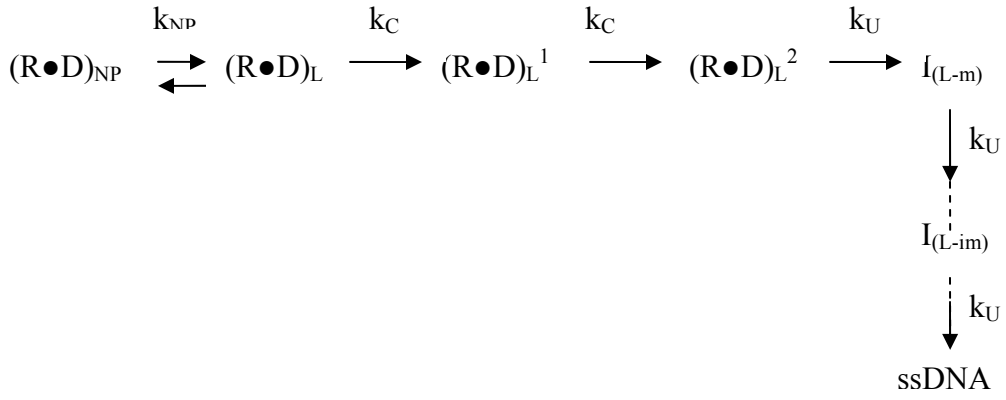

Fig. 4: The reaction scheme of RecBCD unwinding reaction as proposed by Lucius et al. (2004). The notations used are as follows: $(R\bullet D)_{NP}$, the non-productive DNA-enzyme complex; $(R\bullet D)_L$, the productive DNA-enzyme complex. $(R\bullet D)_L^1$ and $(R\bullet D)_L^2$ are two other conformations of the productive complex; k_U, the unwinding rate constant; k_C, rate constants for the extra steps, appearing before the unwinding starts; k_{NP}, the net rate constant of the isomerization of $(R\bullet D)_{NP}$ to $(R\bullet D)_L$; $I_{(L-m)}$ and $I_{(L-2m)}$, are partially unwound DNA intermediates.

By non-linear least square analysis they determined the values of n for different lengths (L) of the duplex, and plotted against the corresponding values of L. The points formed a straight line. Lucius et al. first used a mechanism that consisted of only the unwinding steps with rate constant k_U, and no extra step with rate constant k_C. When the plot of n vs. L was extrapolated to L = 0, it formed an intercept on the Y-axis, while in the ideal case it should have passed through the origin. Then they

introduced 1, 2, or 3 extra steps (h) as shown in Fig. 4, with rate constants k_C, and carried out least square analysis again. They found that with one extra step, the intercept on the Y-axis was reduced, and it improved with two extra steps. Finally, with three extra steps the intercept became negative. According to them, the simulated graphs also fitted their data better with the inclusion of 2-3 extra steps, as shown in Fig. 4. The values of the rate constants of the extra steps were different from those of regular unwinding steps. They repeated the unwinding kinetic studies at different ATP concentrations. Table 1 shows the values of the rate constants and other parameters obtained at different ATP concentrations in this study.

[ATP]	k_U (s^{-1})	k_C (s^{-1})	k_{NP} (s^{-1})	m (bp $step^{-1}$)	h (steps)	mk_U (bp s^{-1})
1.4 mM	176±20	47 ± 2	5.4 ± 0.3	3.6 ± 0.4	3.1 ± 0.1	628 ± 7
416 µM	154±11	39 ± 1	4.3 ± 0.2	3.4 ± 0.2	2.8 ± 0.1	516 ± 5
120 µM	89 ± 7	29 ± 1	3.8 ± 0.2	3.9 ± 0.3	2.9 ± 0.1	343 ± 3
75 µM	54 ± 6	35 ± 8	6.0 ± 0.3	4.2 ± 0.4	3.0 ± 0.6	225 ± 4
37.5 µM	38 ± 1	38	7.2 ± 0.1	3.7 ± 0.1	3	142 ± 2
10 µM	6.4±0.04	-	1.68±0.01	4.25±0.03	0	27.01 ± 0.03

Table 1: **Kinetic parameters determined by Lucius et al. (2004) from non-linear least squares analysis.** These parameters are (see Fig.4) k_U, the unwinding rate constant; k_C, rate constants for the extra steps, appearing before the unwinding starts; k_{NP}, the net rate constant of the isomerization of the non-productive DNA-enzyme complex, $(R{\bullet}D)_{NP}$, to the productive complex, $(R{\bullet}D)_L$; m, the step size; h, the number of extra steps with rate constant k_C; mk_U, the rate of unwinding.

Lucius et al. (2004) found that the values of k_C did not vary with the change of the ATP concentrations. This was in contrast to the unwinding steps. The rate constants of the unwinding steps increased with increasing ATP concentrations, which means the unwinding rate increases with increasing ATP concentrations.

In one experiment, one end of a double stranded DNA was blocked for RecBCD binding, and at the other end, one strand was labeled with Cy3 fluorescence label. As RecBCD starts unwinding and moves away from that end, the fluorescence signal diminishes. A plot of the fluorescence signal vs. time showed that there was a lag time after the start of the reaction and before the start of unwinding. This made this group believe that the two extra steps account for this lag time and they interpreted that two to three ATP independent steps occur before the actual unwinding of a double stranded DNA by RecBCD takes place.

Crystal structure of RecBCD:

In 2004, Singleton et al. determined the crystal structure of RecBCD (Fig. 5). In their structure the enzyme is bound to a blunt-ended DNA hairpin forming the initiation complex. In this complex four base pairs at the end of the DNA are unwound with the 3' end bound to the RecB subunit and the 5' end bound to the RecC subunit. The structure shows how the three subunits are positioned with respect to each other and the position of the DNA strands with respect to the enzyme subunits. Also it suggests the possible path along which the DNA strands could travel once ATP is added and RecBCD starts moving. The DNA strands can pass along two

different channels through the enzyme. The 5' strand passes through the RecC subunit and then through the RecD subunit and then exits. The 3' strand passes through the RecB subunit and then through the RecC subunit. The 3' strand then comes in contact with the nuclease site of RecB and gets cleaved depending on the ATP and Mg^{++} concentrations. The 5' strand also can come in contact with the nuclease site. But it is positioned less favorably with respect to the site and has less chance of getting cleaved when it is in competition with the 3' strand for that site.

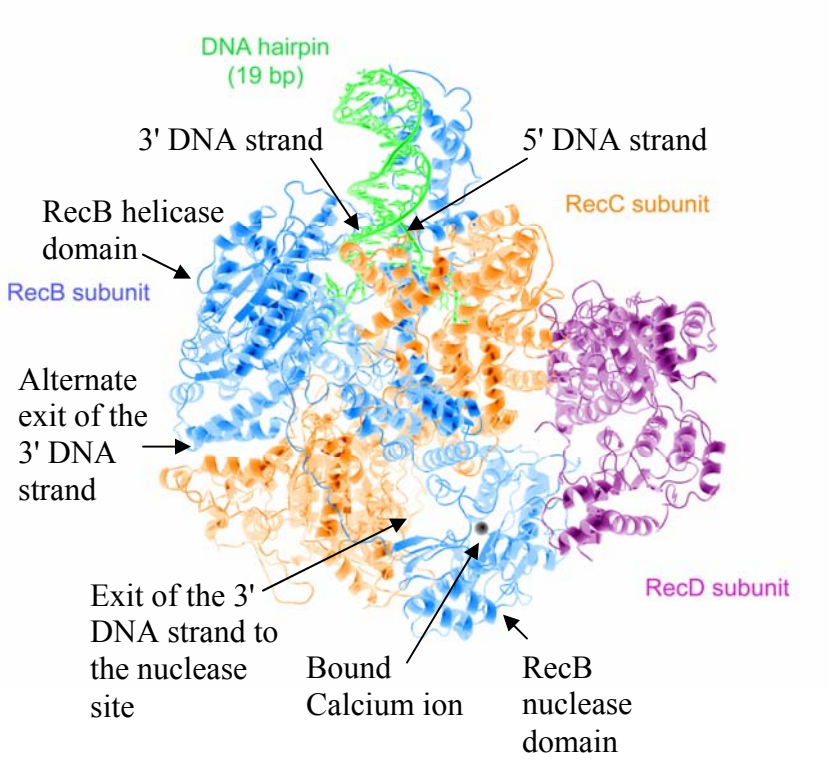

Fig. 5: **Structure of RecBCD enzyme** (figure kindly provided by Prof. Dale Wigley, London Research Institute).

In the structure resolved by these authors, an alpha helix can be seen to block the access of the nuclease site by the 3' strand. In addition to that, there is an alternative exit from the 3' channel of RecC, which passes along the back of the nuclease domain. If the 3' strand uses this exit, it cannot come in contact with the nuclease active site. But nuclease activity does occur, which means, in some or all conditions, the 3' strand takes the exit which is towards the nuclease site, and overcomes the obstruction of the alpha helix. As pointed out by Singleton et al. the helix is connected to the protein by two long flexible linker regions. So it can be moved away clearing the path to the nuclease site. There are two questions that arise here, first, what are the conditions that favor one exit or another from the 3' tunnel? Second, what makes the alpha helix swing away from its resting position?

A brief summary of the present work:

We studied pre-steady state exonuclease activity of RecBCD at four different ATP concentrations with radioactively labeled single stranded oligomers as substrates. We carried out this study as an extension of the work on ATP-stimulated nuclease activity with single-stranded oligonucleotides, done by Chen et al (1998). Although their studies showed a relation between the ATP hydrolysis and nuclease activities, they were not sure about the nature of the requirement for ATP hydrolysis. One of their speculations was that the ATP hydrolysis is directly related to movement along the DNA and indirectly related to the nuclease activity. The movement would enable the DNA to reach to the nuclease active site of the enzyme, where it could be

cleaved. However, they used single stranded oligmers as substrates and there was no previous evidence for ATP-dependent translocation on these substrates. Also, these researchers could see only the end products of the nuclease reaction of the enzyme with the DNA. They could not probe the translocation of the enzyme along the DNA and see intermediates from nuclease cleavages.

We tried to look at the first few steps taken by the enzyme on single stranded oligomers within a one second time period. Reactions were done at saturating enzyme concentrations. A Kintek Rapid Quench Flow instrument was used to carry out reactions at the millisecond level. Reaction mixtures containing the reactants and the products were analyzed by sequencing gel electrophoresis. DNA bands representing the substrates and the products were visualized by phosphor-imaging.

We analyzed the time courses of appearance and disappearance of DNA substrates and the nuclease intermediates and products formed during different time periods ranging from 0-2 seconds. Kinetic data analysis was carried out using the KinTekSim program from the Kintek Corporation. Our studies demonstrate that the ATP-dependent translocation of the enzyme along single stranded oligomers can be compared to the ATP dependent helicase activity of the enzyme on double stranded DNA. Our results agree with the unwinding rate of the enzyme found by Lucius et al. (2004), although both the experiment and the analysis were done in ways completely different from theirs.

MATERIALS AND METHODS:

Labeling of DNA with tritium and isolation:

Cells from a single colony of *E. coli* JM109[pPVSm19] strain were inoculated into 2.5ml of minimal media [1X M9 salts (6% w/v Na_2HPO_4, 3% w/v KH_2PO_4, 0.5% w/v NaCl, 1% NH_4Cl), 0.2% w/v casamino acids, 0.2% w/v glucose, 2mM $CaCl_2$, 0.002% w/v thiamine]. This culture was grown overnight. A 250ml minimal media was inoculated with this culture at 1:200 dilution. The culture was allowed to grow until OD_{600} was 0.1-0.2. Tritium labeled thymidine (1.25ml) [(methyl-^{3}H) thymidine (1mCi/ml)] was then added to the culture and it was allowed to grow for 8 hours. The cells were then harvested and the labeled plasmid DNA was purified using a Qiagen plasmid maxi-prep kit.

Nuclease assay of RecBCD using tritium labeled DNA:

In the nuclease assay of RecBCD, the enzyme was allowed to react with a known amount of tritium labeled linear dsDNA substrates and the amount of small oligonucleotide products was measured. The substrate was mixed in a 20µl reaction mixture containing 50mM TrisHCl, pH 8.5, 10mM $MgCl_2$, 200µM ATP, 0.67mM DTT and 0.2mg/ml BSA in a microcentrifuge tube. RecBCD was added to start the reaction. The reaction was stopped after 10 min by adding 190µl of 20µM EDTA. TCA (100%, 18 µl) was then added to the solution, mixed thoroughly, and then the microcentrifuge tube was placed on ice for 15 min. TCA is known to precipitate the protein and the unreacted DNA (if any). The tube was then centrifuged at the highest

speed for 10min. Most of the supernatant (200µl) was collected from the top slowly without disturbing the invisible pellet at the bottom. The supernatant was transferred to a scintillation vial. About 4ml of scintillation fluid was added to it, mixed thoroughly, and the radioactivity was counted by a scintillation counter.

Purification of RecBCD using an *E. coli* strain overexpressing RecBCD:

Protein expression:

RecBCD was purified from the *E. coli* XL1−Blue strain. This is a *rec*A deficient strain, so it is recombination deficient. The bacterial cell was transformed with the following plasmids:

-● pMS421 – contains streptomycin resistance gene and expresses lac repressor

● pPB520 – contains chloramphenicol resistance gene and expresses RecC

● pPB800 – contains ampicillin resistance gene and expresses RecB and RecD

Over-expression of the enzyme was achieved by using the tac promoter containing a lac operator. The tac promoter is a mixture of the -35 region of the tryptophan promoter and the -10 region of the lacUV5 promoter. This promoter is known to be very strong.

XL1-Blue [pMS421 / pPB520 / pPB800] cells from a frozen stock were grown in LB media containing 100µg/ml of ampicillin, 170µg/ml of chloramphenicol and 50µg/ml of streptomycin overnight. The culture was then inoculated onto LB-agar plates containing the same antibiotics. A single colony was then inoculated in 2ml of LB media and allowed to grow for 10 hrs. This culture (250µl) was then inoculated into 50ml of media. After 10hrs of growth 10ml of this culture was inoculated into 2

liters of media. Each of these media contained all of the three antibiotics. The bacteria in the final media were allowed to grow till OD_{600} was 0.5-0.7. During this time Lac repressor was expressed and it bound to the lac operator and repressed the expressions of RecB, RecC and RecD. When OD_{600} was 0.5-0.7, IPTG was added to the media to induce the repressed promoter. The cells were allowed to grow for 4 hours more during which RecBCD was over-expressed. The culture was harvested at 5000 rpm, by the JA-10 rotor in a Beckman centrifuge, at 10°C for 10 minutes.

Sonication:

The pellet was suspended in buffer A (4ml/ gm of pellets) [See below for the composition of buffer A]. The suspension was divided into 50-60 ml aliquots in plastic tubes and was subjected to sonication. Sonication was done by Branson Sonifier sonicator at 60% output and 30% duty cycle. Each tube was sonicated for 30 seconds, left on ice for some time to cool it down and then sonicated again for 30 seconds, and it was repeated six times, making the total time for sonication 3 minutes for each tube. The sonicate was centrifuged for 45 min at 14K rpm at 4°C, by the JA-20 rotor in the Beckman centrifuge. The supernatant was collected and was subjected to ammonium sulphate precipitation.

Ammonium sulphate precipitation and dialysis:

Volume of the supernatant was measured. Calculated amount (0.282g/ml of supernatant) of $(NH_4)_2SO_4$ was weighed and was ground into powder. It was added in small amounts to the supernatant with continuous stirring, allowing sufficient time for

dissolving each small fraction. Dissolving $(NH_4)_2SO_4$ caused a portion of the protein to precipitate, making a turbid solution. When all the salt was dissolved the stirring was continued for half an hour more to allow as much protein to precipitate as possible. This suspension was centrifuged at 14K rpm at 4°C for 45 min, by the JA-20 rotor. RecBCD is known to be present in the pellet, which was then collected. The protein in this form is quite stable and could be stored at 4°C overnight. Also the supernatant was stored and tested by nuclease assay and by gel electrophoresis later for the presence of trace amounts of RecBCD.

The pellet was dissolved in a small volume of buffer Q [See below for the composition of buffer Q]. This was dialyzed for 8 hours against a total of 4 liters buffer Q, 2 liters of buffer at a time, each time for 4 hrs. It was then ready to be loaded onto a Q-sepharose column.

Q-sepharose column preparation and loading:

Q-sepharose was obtained from Pharmacia Biotech. Q-sepharose beads were stored in 20% ethanol with volume ratio of Q-sepharose: ethanol-water = 4:1. For 2 liters of culture we wanted to make a 50ml column. The ethanol was washed out with water and then the Q-sepharose bead was washed a few times with buffer Q. Finally a suspension of Q-sepharose in buffer Q was added to the column along a glass rod. Sufficient time is allowed for the beads to settle down forming a compact column. A piece of filter paper of the same area as that of the top surface of the column was laid on that surface. This was done to prevent the buffer drops from affecting the uniformity of the bead surface.

A three way luer valve was connected at the top entrance of the column in an air tight manner. A similar valve was also connected to the bottom exit of the column. The upper valve was connected by a polyethylene tubing to a beaker containing the buffer. The connection between the tubing and the valve and the valve and the column should be airtight for the siphoning effect to work. The column was equilibrated with five column volumes of buffer Q.

The dialyzed protein was loaded on the column and then washed with five column volumes of the low salt buffer (Buffer Q + 0.15M KCl). The column was then eluted with a gradient of 5 column volumes of the low salt buffer and 5 column volumes of the high salt buffer (Buffer Q + 0.6M KCl). The eluate was collected in 1.5-2.0ml fractions. The OD_{280} of these fractions was measured and a graph of OD_{280} vs. sequence number of the tube is made. A protein peak in the washing and two peaks in the elution were found. We tested the tubes in and around the peaks for the presence of any ATP dependent exonuclease activity. For this, we made nuclease reaction mixtures (as described above) in microcentrifuge tubes in duplicates. One tube in each pair contained ATP, and the other did not contain any ATP. Protein solution (1μl) from every elution tube to be tested was taken and added to both microcentrifuge tubes in a pair. Tubes containing RecBCD showed much higher amount of reaction in the microcentrifuge tubes containing ATP, than in the tubes not containing ATP.

The tubes right after the main peak in the elution contained such ATP dependent exonuclease activity, which indicated the presence of RecBCD in those

tubes. Finally presence of the protein was confirmed by analyzing samples from those tubes by polyacrylamide gel electrophoresis (PAGE).

Second ammonium sulphate precipitation and dialysis:

The fractions containing RecBCD were pooled and the volume was measured. Calculated amount of $(NH_4)_2SO_4$ (0.39 g/ml) was dissolved slowly as described above. The precipitated protein, thus formed, was centrifuged as described above. RecBCD is known to be present in the pellet, which was then dissolved in buffer C [See below for the composition of buffer C]. The protein solution was dialyzed against 2 liters of buffer C. It was then ready to be loaded onto the Hydroxylapatite column.

Hydroxylapatite column preparation and loading:

We made a 20ml column for the second chromatographic separation of the protein. DNA grade Hydroxylapatite powder was bought from BioRad. Weighed amount [8 gm] of powder was suspended in 10mM phosphate buffer. It was then washed with the same buffer several times to get rid of the fines. Finally a suspension of hydroxylapatite was added to a glass cylinder as described above forming a 20ml column. A connection to the buffer container was made through valves. The column was then equilibrated with 5 column volumes of buffer C.

The protein solution was added to the column by siphoning. The column was then washed with 5 column volumes of buffer C. It was then eluted with a gradient of 5 column volumes of buffer C and 5 column volumes of the buffer C gradient buffer.

The eluate was collected in fractions of approximately 1ml. As before, a graph of OD_{280} vs. sequence number of the fraction was made. A protein peak in the washing and two peaks in the elution were obtained. RecBCD was found to be present in the first of the two peaks of the elution by exonuclease study and gel electrophoresis.

Finishing and storing of the final protein prep:

RecBCD found in the last step was quite sufficiently pure for our studies. The fractions containing the protein were pooled and dialyzed against 2 liters of buffer D containing 50% glycerol [See below for the composition of buffer D. The protein solution in this form could be stored in -20°C and -80°C for a long time. We distributed the solution in 250µl aliquots in 1.5ml microcentrifuge tubes and stored some of them in -20°C and the rest in -80°C. The final concentration of the purified protein was 3.2µM. Fig.6 shows three subunits of RecBCD in a SDS-PAGE gel.

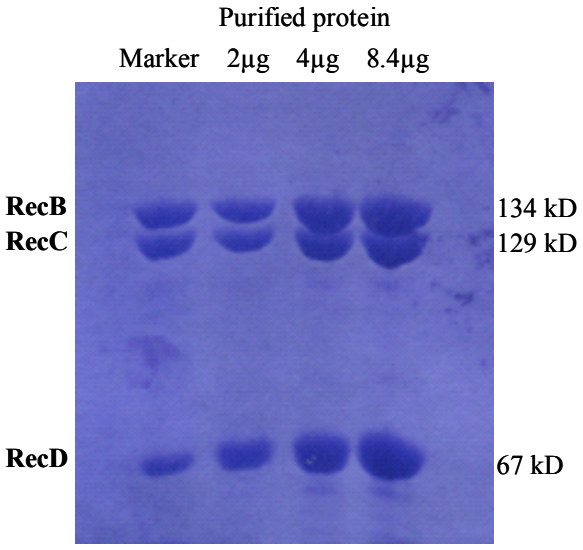

Fig.6: Purified RecBCD (SDS-PAGE)

Following is a list of all the buffers used in RecBCD purification and their compositions:

Buffer A:	50 mM TrisHCl, pH 7.5
	0.2 M NaCl
	10% sucrose
	10 mM mercaptoethanol
	1 mM EDTA
Buffer Q:	20 mM bis-Tris propane-HCl, pH 6.9
	0.1 mM EDTA
	0.1 mM DTT
	10% (v/v) glycerol
Buffer C:	25mM KPO_4, pH 6.9
	1mM DTT
Buffer D:	10mM KPO_4, pH 6.9
	0.1 mM EDTA
	0.1 mM DTT
	50% glycerol

Substrates used in the exonuclease study:

Single stranded oligonucleotides, 40 bases long, were bought from Invitrogen. We worked with three different sequences, pAG1s, pAG1rs and pAGC20rs as shown in Table 2. The oligomers were gel purified by the manufacturer. They were dissolved in TE buffer and stored at -20°C. We also purchased four more oligomers, pAG135, pAG128, pAG120 and pAG112 of lengths 35 bases, 28 bases, 20 bases and 12 bases respectively. We ran these oligomers in a single lane of a sequencing gel to use them as size markers.

Oligomers	Sequences	Bases
pAG1s	TGTCGTTGAG GACCCGGCTA GGGTTGCCTT ACTGGTTAGC	40
pAG1rs	GCTAACCAGT AAGGCAACCC TAGCCGGGTC CTCAACGACA	40
pAGC20rs	GCTAACCAGT AAGGCAACCC CACCAGCCTA GCCGGGTCCT	40
pAG135	TGTCGTTGAG GACCCGGCTA GGGTTGCCTT ACTGG	35
pAG128	TGTCGTTGAG GACCCGGCTA GGGTTGCC	28
pAG120	TGTCGTTGAG GACCCGGCTA	20
pAG112	TGTCGTTGAG GA	12

Table 2: **Oligonucleotides used for the exonuclease reactions.**

For determination of the concentration, spectrophotometric absorption of a diluted solution of the oligomer at λ_{260} was taken. We then calculated the concentration by using the millimolar extinction coefficient (OD/μmol), provided by the manufacturer for the particular oligomer, as shown below:

$C = (A_{260} \text{ X } d) / E$

Where, A_{260} = Spectrophotometric absorption of the diluted solution at λ_{260}

E = Millimolar extinction coefficient of the oligomer (OD/μmol)

d = Dilution factor

Labeling of the oligomer substrates:

The 5' end of the oligomer was labeled with ^{32}P by using T4 polynucleotide kinase (T4 PNK) from New England Biolabs Inc. and γ-^{32}P 5'-end labeled ATP (3000 Ci/mmol) from Amersham Biosciences. PNK buffer (1X), oligomer solution (5μl), γ-^{32}P ATP (165nM) and water (77μl) were mixed together in a microcentrifuge tube. T4 PNK (30 units) was added to start the reaction. The tube was incubated in a 37 °C water bath for 1 hour. After the incubation, during which the labeling reaction should be complete, the tube was taken out and the mixture was subjected to purification as described below.

The 3' end was labeled by using terminal transferase from New England Biolabs Inc. and α-^{32}P dideoxy ATP (3000Ci/mmol) from Amersham Biosciences. A 97μl labeling mixture containing NEbuffer 4 (1X), $CoCl_2$ (250μM), oligomer solution (5μl), α-^{32}P dideoxy ATP (165nM) and water (67μl) was prepared in a microcentrifuge tube. Terminal transferase (60 units) was added to start the reaction

and the tube was incubated for 1 hour in a 37°C water bath. After the reaction the mixture was subjected to purification as described below.

Quantitation of the labeled oligomers:

After labeling oligomers were purified using the Qiaprep Spin Miniprep kit. This purification involves selective binding of DNA to a silica gel column, washing away any unreacted ATP or protein with 70% ethanol, and then eluting the DNA from the column with 10mM Tris-HCl (pH 8.5). Some of the labeled DNA is lost in this process.

We started with a known concentration of the oligomer in the labeling reaction mixture (D_o). We measured the loss of the total radioactivity due to purification of the labeling mixtures. For this, we diluted 0.5µl of the mixture, before purification and after purification, to 200µl with water. Then 4ml of scintillation fluid (BioSafe II, purchased from Research Products International Corp.) was mixed with this diluted mixture in a scintillation vial thoroughly. The radioactivity of this mixture is counted with a Beckman-Coulter LS-6500 multipurpose scintillation counter, which gives the value of radioactivity in counts per minute (cpm). This loss of radioactivity could be due to the loss of the ^{32}P labeled DNA or the loss of radioactive ATP. So we measured the percentage radioactivities of the labeled DNA in the initial and the final mixtures. For this, we placed 0.5µl drops of labeling mixtures, before purification and after purification on 3″/2″ pieces of Baker-flex polyethyleneimine cellulose thin layer chromatography (TLC) paper (J.T. Baker) and dried the drops. Then we ran a thin layer chromatography with 1M sodium phosphate (NaH_2PO_4, pH 3.5) buffer as the

mobile phase. Thus we could separate ATP, free inorganic phosphate and labeled DNA in the chromatograms. The chromatograms were dried and were exposed to storage phosphor screens. These screens were scanned by the Storm phosphor-imager. Following is an image of the TLC plate, scanned by the storm phosphor-imager.

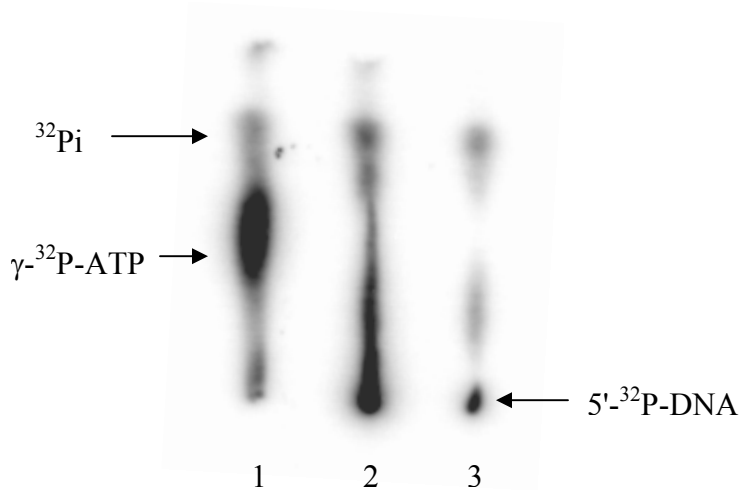

Fig 7: Thin-layer chromatographic separation of three samples from the DNA labeling mixture. (1) before starting the polynucleotide kinase reaction, (2) after the labeling reaction, and (3) after the purification.

It can be seen in the scanned image that radioactive ATP, ^{32}P-inorganic phosphate, and labeled DNA appeared as three different spots. These spots were analyzed by the Imagequant program and the relative radioactivities of these spots were determined. Finally we calculated the concentration of the labeled oligomer in the final mixture (D_{final}) using the following equation:

$$D_{final} = D_o \text{ X } (R_{final} / R_{ini}) \text{ X } (T_{final} / T_{ini})$$

Here, R_{final} = Final radioactivity

R_{ini} = Initial radioactivity

T_{final} = Percentage radioactivity of the labeled DNA with respect to the total radioactivity in the final purified mixture

T_{ini} = Percentage radioactivity of the labeled DNA with respect to the total radioactivity in the initial mixture

Table 3 shows a list of the values of the above parameters for two labeling reactions and the concentrations determined from them.

D_o (μM)	R_{ini}	R_{final}	T_{ini}	T_{final}	D_{final} (nM)
2.31	893181	139127	48.16	35.55	265.60
2.09	817037	145039	43.86	33.33	282.1

Table 3: Determination of the final concentrations of the radioactively labeled and purified oligomers.

Experiment with Kintek Rapid Quench Flow (RQF) Instrument:

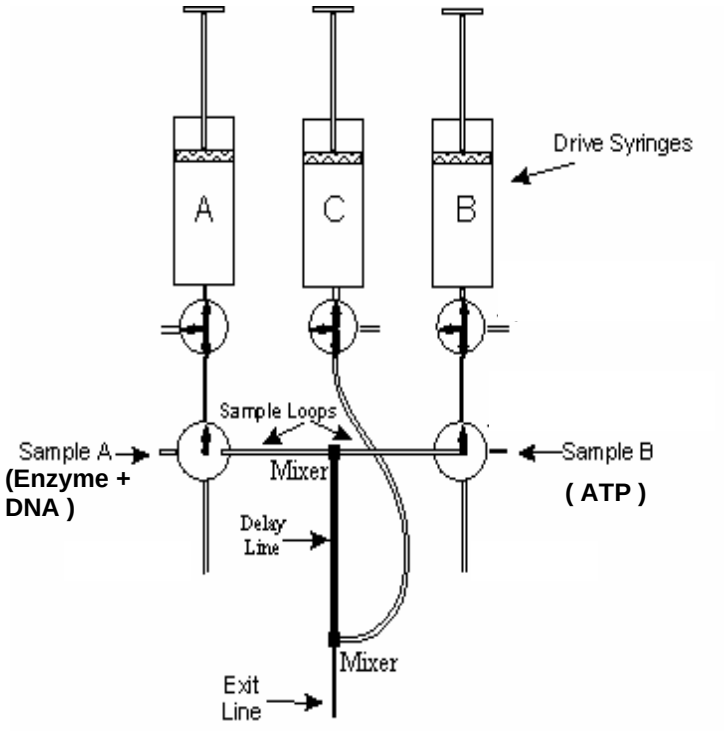

Fig. 8: **Kintek Rapid Quench Flow Instrument.**

Above, there is a diagram of the RQF instrument (Fig. 8). There are three buffer chambers of 5-6ml capacity. Chambers A and B were filled with 50mM Tris buffer (pH 7.5) and chamber C was filled with 400mM EDTA solution. The EDTA solution was used to quench the exonuclease reaction. There are two sample loops with corresponding loading ports. For most experiments, labeled DNA substrate in nuclease reaction buffer (25mM Tris acetate, 8mM Mg-acetate, 1mM DTT, pH 7.5) was placed in sample A loop, and ATP dissolved in reaction buffer was placed in

sample B loop with the help of 1ml plastic syringes. The instrument is connected to a computer which is used to start the reaction and it controls the time of the reaction depending on user inputs.

When the instrument is set to start the reaction, the pistons in the buffer chambers move downward with high speed. The buffer from chambers A and B is forced out and it pushes the reactants in sample loops A and B into a reaction loop. There are 7 different reaction loops with different volumes, numbered from 1 to 7. These seven loops are used to carry out fast reactions of different reaction time periods as described in the next section.

The particular reaction loop used for the reaction is determined before the user sets the instrument to start the reaction. The user is asked to set a reaction time, and then the computer determines the number of the reaction loop needed for that reaction. The user sets the reaction loop and then pushes the button to start the reaction.

The two reactants are mixed in the reaction loop and the reaction takes pace. On exiting the reaction loop, the reaction mixture gets mixed with the quench solution from chamber C in the exit line and the reaction stops.

Calibration of the RQF instrument:

The precision of the reaction time, achieved by this instrument, depends on the calculated movement of a motor. The computer controls the movement of the motor, along with the instrument as a whole. When a reaction is started, the computer sends an impulse to the motor. The motor moves one step for each impulse. One revolution of the motor is made up of 5000 such steps. The stepwise movement of the motor pushes the pistons in the syringes. As a result the liquid in the syringe is pushed out, which in turn pushes the reactants out of the sample loops and through the selected reaction loop.

Reaction time period is the time during which the two reactants remain inside the reaction loop, getting mixed with each other and undergoing the reaction. For small time periods it depends on the length of the reaction loop and speed of the motor in revolutions per minute. The instrument uses a minimum motor speed of 180rpm. In each reaction loop, this minimum speed gives the longest time of reaction available for that loop. However, there is no such limit for loop 7, which is the longest among the reaction loops. For a long reaction time, the motor moves and pushes the reactants into the reaction loop and the reaction starts. The motor then pauses till the end of the reaction time period. Then, a second movement pushes the reaction mixture out of the reaction loop and it gets mixed with the quench buffer and the reaction gets stopped.

The user needs to calibrate the instrument before it is used for quench flow runs. This includes:

(1) Measuring the volume of each reaction loop

(2) Measuring the number of steps needed to completely expel the content of each reaction loop

(3) Measuring the volume of liquid delivered by the two drive syringes per revolution of the motor

(4) Calibrating the instrument by providing these values to the computer.

These measurements were done as described in the instruction manual of the Kintek RQF instrument. As these values are entered in the computer, it saves the values and uses them to calculate the maximum reaction time for each loop. Also, during a quench flow reaction, when the user enters the reaction time, the computer uses the above values to calculate the required speed of the motor and gives out the number of reaction loop to be used.

The relation between the time (t), the volume of the reaction loop (V) and the flow rate (F) is expressed as:

$t = V \times 60 / F$ (μl)/ (μl/sec),

Flow rate (F) is expressed as:

F = Volume per revolution X Run speed (r.p.m)

Reactants used in the quench flow reactions and reaction conditions:

Following is a list of the different combinations of reactants used for the exonuclease reaction:

	Combination	Sample A	Sample B
	1	DNA + RecBCD + Mg^{++}	ATP + Mg^{++}
	2	DNA + RecBCD + Mg^{++}	ATP + unlabeled DNA trap + Mg^{++}
	3	DNA + RecBCD + unlabeled DNA trap + Mg^{++}	ATP + Mg^{++}
	4	DNA + Mg^{++}	RecBCD + ATP + Mg^{++}

Table 4: **Combination of reactants used for the exonuclease study by Kintek Rapid Quench Flow Instrument.**

We used 15-22nM of DNA and 8mM of Mg++ for the reactions. Concentration of the enzyme was 160-384nM depending on the reaction set up. Four different ATP concentrations, 20μM, 50μM, 200μM and 1mM were used. In the final reaction mixture, these concentrations become 10μM, 25μM, 100μM and 500μM respectively. The DNA trap was used in concentrations of 100 to 300 times that of labeled DNA reactant. We used the same oligomers as the DNA traps as those used as the reactants. The only difference was that the reactant DNA was labeled, while the trapping DNA was unlabeled.

Sequencing gel electrophoresis:

Acrylamide-bisacrylamide solution for polyacrylamide gel was bought from Bio-Rad. We used Sequi-Gen Nucleic Acid Sequencing Cell (Bio-Rad) gel apparatus for running the sequencing gel electrophoresis. The sequencing gel was made by mixing 15% (37.5:1) Acrylamide-bisacrylamide solution, 42gms of urea (7%) with 1% TBE buffer (10.8gm Tris base, 5.5gm boric acid, 4.5gm EDTA in 1 litre deionized water) to a total volume of 100ml. TEMED (150µl) and APS (300µl) were added to 100ml of the gel solution to start the polymerization reaction.

The enzyme reaction mixture containing the reactant, intermediates and products from each time point was run in a lane of a sequencing gel. The electrophoresis was run at 1500 V at 50°C using 1% TBE buffer. The reaction mixture contained a high concentration of salt, which affects the pattern of the ladder of bands in the lanes of the gel. To avoid this, salt solutions of similar concentration were loaded in the lanes flanking the lanes containing the reaction mixtures. We used 400mM EDTA solution to load in these flanking lanes.

It is very important to clean the gel plates before a run. The plate can be cleaned using bleach and then washed thoroughly with water. It is then dried with a clean paper towel. After washing we coated the back plate containing the buffer chamber with Safetycoat (a non-toxic glass coating from J.T.Baker). For coating, 5ml of Safetycoat is placed at the center of the plate. Then it is gently spread on the entire surface of the plate with a clean paper towel. It is then allowed to air dry for a few minutes. The surface is then gently wiped off with a damp paper towel.

A thorough cleaning of the back plate with 10N KOH was carried out from time to time after a few runs. Proper care needs to be taken during using 10N KOH, because this is very corrosive and can cause harm to the plastic parts of the gel apparatus. For safe handling paper towels soaked with the alkali solution is laid over the plate surface. That way the solution cannot come in contact with other parts of the gel apparatus except the plate surface. After 2-5 hours the paper towels are removed and the plate is rinsed with water. It is then cleaned with bleach and washed thoroughly with water. The plate is then dried and freshly coated with Safety coat as mentioned before.

After running the electrophoresis, the gel is allowed to become cool before pulling apart the two gel plates. If the gel is hot it tends to stick on both the plates and breaks down into pieces when plates are pulled apart. The gel also shows this sticking problem when the plates are not cleaned thoroughly as described above.

Exposing to phosphor-imaging screen and scanning by Storm phosphor-imager:

When the two gel plates are separated, the gel remains stuck to the non coated plate. The plate with the gel is soaked in 10% acetic acid for about 15min. This is done to remove urea from the gel. Also the gel gets separated from the glass plate in this process. It is then placed on a filter paper and is dried by a FisherBiotek model 583 gel dryer. Two pieces of Whatman DE-81 anion exchange chromatography paper (grade DE-81) are used to catch any radioactive ATP or DNA that may be transferred from the gel to the surface underneath. The gel is dried at 90°C for 50 min and then it

is exposed to a phosphorimager screen. After 4 days of exposure the screen is scanned by a Storm phosphorimager.

ImageQuant Software:

ImageQuant Software is used to open and edit the image scanned from a phosphorimager screen. We can increase or decrease the zoom size. The brightness of the image can be adjusted to see the bands more clearly. Also, small areas corresponding to a band or a spot can be selected and the total pixel in that area can be calculated by this program.

Fragment analysis software:

First, the Fragment analysis program is opened, and then ‘open image’ option from file menu is clicked. The image that is needed to be analyzed is opened. The color property may need to be adjusted to open the image. The computer is generally set at 32 bit color. The Storm computer contains another option called 256 colors. In order to open an image by fragment analysis program, the computer is to be set at 256 colors. For this, we can go to ‘properties’ by a right click on the desk-top. Then, we can go to settings, and then select 256 colors.

Sometimes brightness of the opened image becomes critical to the relative quantitation of the bands. The brightness scale should be adjusted so that all the bands can be clearly seen, and there is no overlap between two or more bands. There is an option to adjust the brightness in fragment analysis, but we found it to be less

complicated to do it by the ImageQuant program, save it there, and then open the image by Fragment analysis in order to analyze it.

The program automatically guides the user through finding lanes in a picture of gel, finding bands and then quantitating the bands. The program automatically finds the bands and puts small rectangles encompassing the bands. The user may need to do small adjustments such as deleting the rectangles put in the wrong place, or using the semiautomatic or manual band creation option to select the bands undetected by the program. If there is a lane containing size markers, then that lane number and information about the marker bands can be entered in one of the steps during lane finding and band finding. The program uses the information obtained from the marker lane to calculate the size represented by each band.

After finding the bands, the user can ask the program to show the report in a table form. The report shows actual pixel volumes of the bands. Also in every lane, the percentage radioactivity for each band with respect to the total radioactivity of that lane is calculated. The report also shows the size or weight represented by each band calculated from the marker bands. The initial concentration of the substrate for each reaction time point is known. This is proportional to the initial radioactivity of the substrate. Again, the initial radioactivity is equal to the final total radioactivity of the substrate, intermediates and products. So the radioactivity of each substrate, intermediate or product band is proportional to their actual concentrations in the reaction mixture. So we can get the relative concentrations of the substrate and the products for each time point from the percentage radioactivity of the corresponding bands in the corresponding lane.

RESULTS:

Exonuclease activity at different RecBCD to DNA ratio at 1mM ATP:

Our aim was to study the binding of the enzyme to the DNA and to determine the best RecBCD/DNA ratio to work with. We took a known concentration of DNA and allowed it to react with different concentrations of the enzyme. Single turnover pre-steady state exonuclease reactions were carried out for 60ms with 32nM DNA and different concentrations (0-700 nM) of RecBCD. The enzyme was allowed to bind to the DNA for 3-4 minutes, and this was mixed with ATP to start the reaction. Samples from the quenched reaction mixture were loaded on a sequencing gel (Fig. 9) and DNA bands were quantitated. Percentage radioactivities of one of the intermediates at each time point were plotted against the corresponding enzyme concentration (Fig. 10). It can be seen that the amount of reaction reaches a maximum at approximately 2:1 RecBCD/DNA ratio. A significant fraction of the DNA remains unreacted at this ratio and even with a very high enzyme to DNA ratio.

We suggest that the ratio (RecBCD:DNA 2:1) indicates the stoichiometry of binding of the enzyme to the DNA ends. One enzyme molecule can bind to each of the ends of a single stranded oligomer, with two enzyme molecules per oligomer. However, not all of the DNA molecules go into the nuclease reaction. Perhaps, some of the bound enzyme molecules cannot start a nuclease reaction. Either, the bound

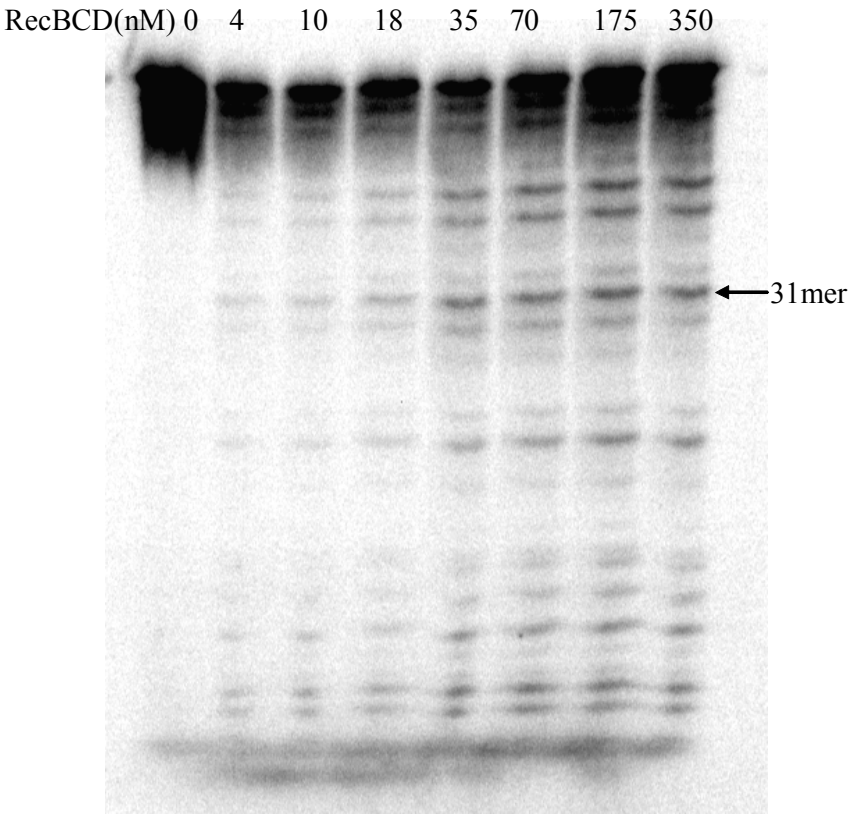

Fig. 9: **Exonuclease activity of RecBCD at different enzyme to DNA ratio.** Sequencing gel image of the exonuclease activity of RecBCD at different enzyme to DNA ratio in 25mM Tris-acetate (pH 7.5), 1mM DTT, 8mM Mg^{++} and 1mM ATP concentrations. Each lane represents the same reaction time period, 60msec. The DNA substrate is the oligomer pAG1s, and it is radioactively labeled at the 5′ end. The substrate concentration for each lane is 15.5nM. Concentration of enzyme varies from 0 to 350nM. We selected one intermediate (31mer) and plotted the percentage of this intermediate against the corresponding enzyme to DNA ratio (shown in Fig. 10).

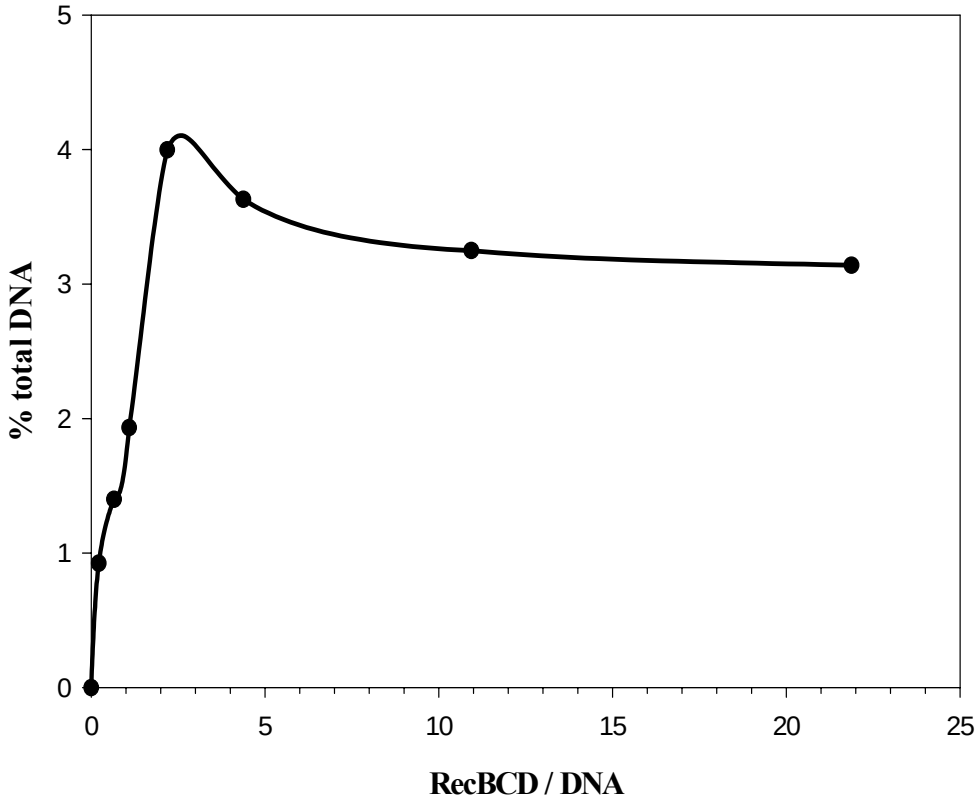

Fig. 10: Percentage of the 31mer intermediate at different enzyme : DNA ratio. Plot of the percentages of the 31 mer intermediate of the exonuclease reactions done at different enzyme to DNA ratio. Percentage values were obtained by the quantitation of the DNA bands of the sequencing gel image (shown in Fig. 9) by the fragment analysis software.

enzyme forms a complex with the DNA which is inactive with respect to the nuclease activity, or, a fraction of the enzyme dissociates from the bound DNA. We also consider the possibility that both of these incidents contribute towards the presence of the unreacted DNA.

Interaction of RecBCD with the labeled DNA in the presence or absence of an unlabeled DNA trap:

In all subsequent exonuclease reactions, the enzyme was almost ten times more concentrated than the DNA. This was done to make sure that all DNA ends are occupied with the enzyme and we get maximum reaction out of the DNA concentration that we used. Since there were excess free enzyme molecules in the solution, they could interfere with the exonuclease reaction that we intended to study. So in some of our reactions we used a large excess of unlabeled DNA oligomers to trap the free enzyme molecules. We used 100-300 times excess of the unlabeled DNA than the labeled oligomers. We carried out three sets of exonuclease reactions, consisting of three sets of time points, to verify the effectiveness of the unlabeled DNA as a trap.

The first reaction was the control, where the enzyme was incubated with labeled DNA and was used as reactant A. ATP was used as reactant B. No trap was used in this reaction. In the second reaction, the enzyme was incubated with the labeled DNA and the mixture was used as reactant A. A mixture of unlabeled DNA trap and ATP was used as reactant B. In the third reaction, the enzyme was incubated with a

mixture of the labeled and the unlabeled DNA and was used as reactant A, while ATP was used as reactant B.

The results are shown in Figures 11, 12, and 13. In the first and the second reactions (Fig. 11), there is enough time for the enzyme to bind at the end of the labeled DNA, before the start of the nuclease reaction. In the simple case of the first reaction (Fig. 11, lanes 2-6), ATP is added to start the reaction. Presumably, all or some of the bound enzyme molecules start moving along the DNA and start creating exonuclease reaction products. In the second reaction (Fig. 11, lanes 7-10), however, a large excess of unlabeled DNA is added along with ATP. So, as ATP binds to the enzyme, the excess unlabeled DNA interacts with the free enzyme in the solution.

In the third set of reactions (Figures 12 and 13) the enzyme is incubated with the labeled DNA and a much higher concentration of the unlabeled DNA. This is another control reaction, which is done to verify if the unlabeled DNA can interact with the enzyme as well as the labeled DNA. When pre-incubated with the enzyme before the start of the reaction, both kinds of DNA should compete with each other for binding with the enzyme at their ends. When the concentration of the added unlabeled DNA is more than that of the labeled DNA and even more than that of the enzyme, not all of the labeled DNA can have enzyme molecules to bind to. At a sufficiently high concentration of the unlabeled DNA, almost all of the labeled DNA can be free of enzymes.

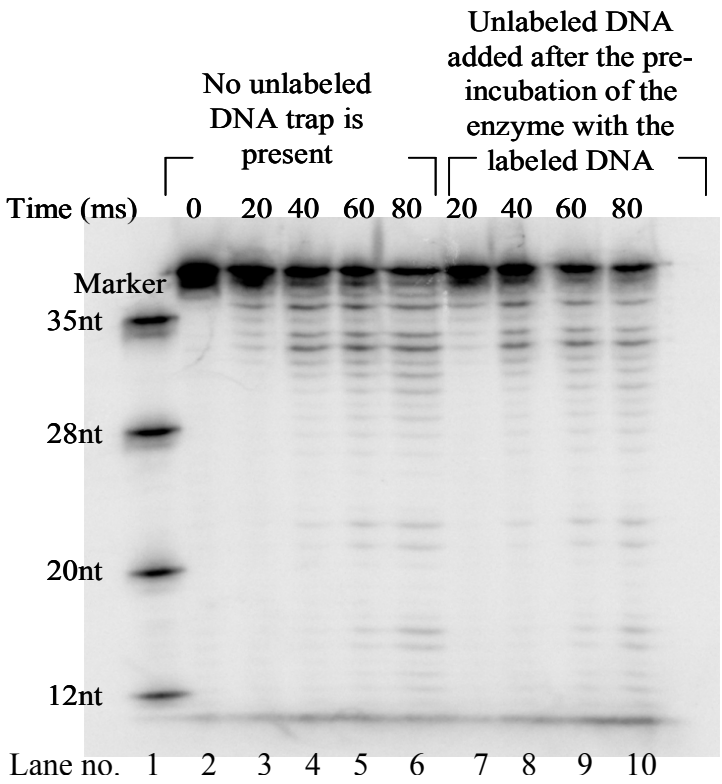

Fig. 11: Exonuclease reaction in the presence or absence of 250 times more concentrated unlabeled DNA trap. Sequencing gel image of the exonuclease reaction of RecBCD with a 5′-end labeled DNA substrate (oligomer pAG1s) in the presence or absence of 250 times more concentrated unlabeled DNA trap. The labeled DNA was pre-incubated with the enzyme. Lanes 1-5 represent the reaction where ATP was added to start the reaction. Lanes 6-9 represent the reaction where the unlabeled DNA was added along with ATP. Reactions were carried out at 25 ºC in 25mM Tris-acetate (pH 7.5), 1mM DTT, 8mM Mg^{++} and 1mM ATP. The enzyme and substrate concentrations were 384nM and 17.5nM respectively.

At first, we used a concentration of the unlabeled DNA which was almost 25 times more than the concentration of the labeled DNA. Samples from the reaction output were subjected to the sequencing gel electrophoresis. The result (Fig. 12) shows that when we included this trap in reactant A along with the enzyme and the labeled DNA, the nuclease digestion of the labeled DNA was reduced. So clearly the unlabeled DNA competed with the labeled DNA for reacting with the enzyme.

Next, we increased the concentration of the trap from 25 to almost 250 times the concentration of the labeled DNA. Our aim was to use a concentration of the unlabeled DNA that would outnumber the labeled DNA completely in a competition for reaction with the enzyme. The result (Fig. 13) shows, in fact, the labeled DNA did not undergo any nuclease digestion when the above concentration of unlabeled DNA was included in reactant A. When the same concentration of the trap was included in reactant B (Fig. 11), there was no significant reduction of nuclease activity as compared to the control reaction.

Subsequently, we used a concentration of the unlabeled DNA, which was 100-300 times more concentrated than the labeled oligomer for our reactions.

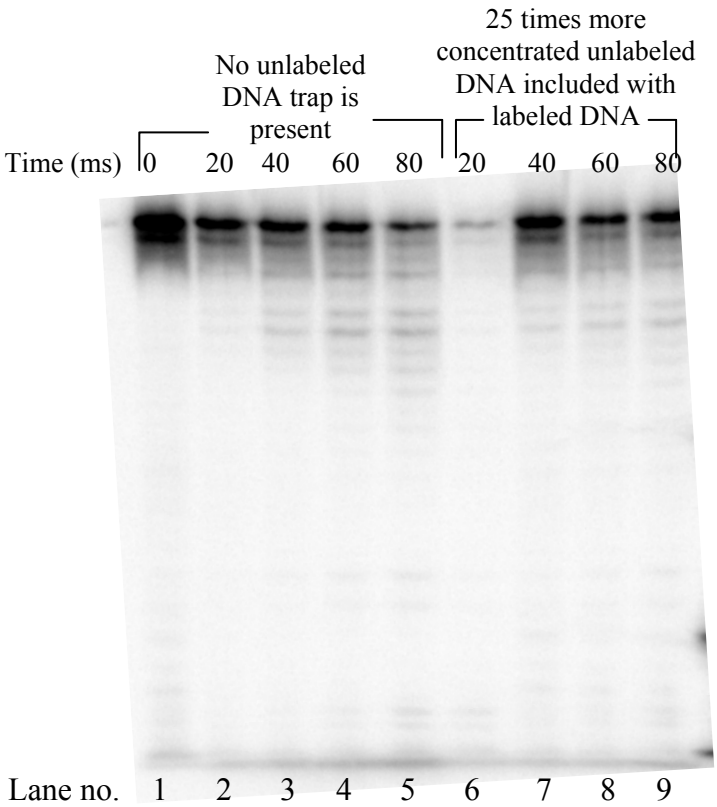

Fig. 12: Exonuclease reaction in the presence or absence of 25 times more concentrated unlabeled DNA trap. Sequencing gel image of the exonuclease reaction of RecBCD with a 5′-end labeled DNA substrate (oligomer pAG1s) in the presence or absence of 25 times more concentrated unlabeled DNA trap. Lanes 1-5 represent the reaction where the labeled DNA was pre-incubated with the enzyme and ATP was added to start the reaction. Lanes 6-9 represent the reaction where both the unlabeled and the labeled DNA were mixed together with the enzyme and pre-incubated before the reaction. Reactions were carried out at 25ºC in 25mM Tris-acetate (pH 7.5), 1mM DTT, 8mM Mg^{++} and 1mM ATP. The enzyme and substrate concentrations were 384nM and 17.5nM respectively.

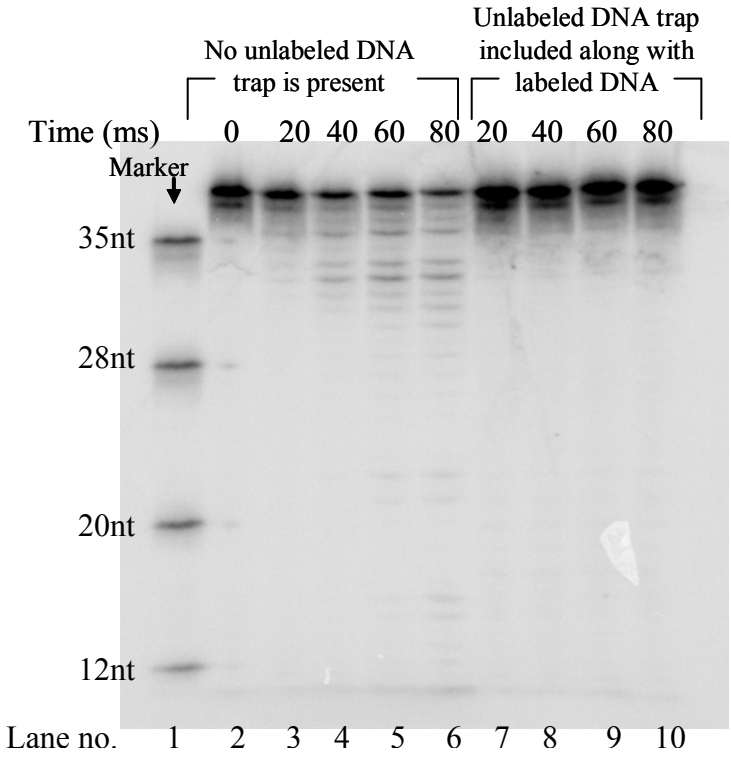

Fig. 13: Reaction of the labeled DNA with the enzyme suppressed by the unlabeled DNA trap. Sequencing gel image of the exonuclease reaction of RecBCD with a 5′-end labeled DNA substrate (oligomer pAG1s) in the presence or absence of 250 times more concentrated unlabeled DNA trap. Lanes 1-5 represent the reaction where the labeled DNA was pre-incubated with the enzyme and ATP was added to start the reaction. Lanes 6-9 represent the reaction where both the unlabeled and the labeled DNA were mixed together with the enzyme and pre-incubated before the reaction. Reactions were carried out at 25ºC in 25mM Tris-acetate (pH 7.5), 1mM DTT, 8mM Mg^{++} and 1mM ATP. The enzyme and substrate concentrations were 384nM and 17.5nM respectively.

Exonuclease reaction of RecBCD with 40 nucleotide single-stranded oligomers of three different sequences:

We carried out exonuclease reactions between RecBCD and 40 base oligomers of three different sequences. In all of these reactions the enzyme was incubated with the DNA and it was in reactant A, while ATP was in reactant B.

The enzyme is known to move along double-stranded DNA very rapidly (500-1000 bp/s) [Roman et al. (1992), Bianco et al. (2001), Lucius et al. (2002)]. In earlier studies final products of the nuclease reaction were observed only after the travel of the enzyme along such short oligonucleotides was completed [Chen et al. (1998)]. In the present study, we allowed the reaction to proceed for only 10-2000 msecs, and stopped the journey of the enzyme midway along the DNA strand. By using radioactively labeled DNA substrates, carrying out reactions by a rapid quench flow instrument, analyzing the products by sequencing gel electrophoresis and then by phosphorimaging, we have been able to visualize the intermediate DNAs of the exonuclease reaction. Results of these experiments are shown in Fig. 14a and 14b.

There were a couple of features that can be seen in the sequencing gel images of the exonuclease time courses of all three sequences. First, the first intermediate band that can be seen in all three sequences is the 38 nucleotide band instead of the 39 nucleotide band (in order to know the sizes of the intermediates, we used a mixture of four oligonucleotides of different lengths as size markers). This means that the first nuclease cut occurs after 2-3 nucleotides from the 3' end and not after the first

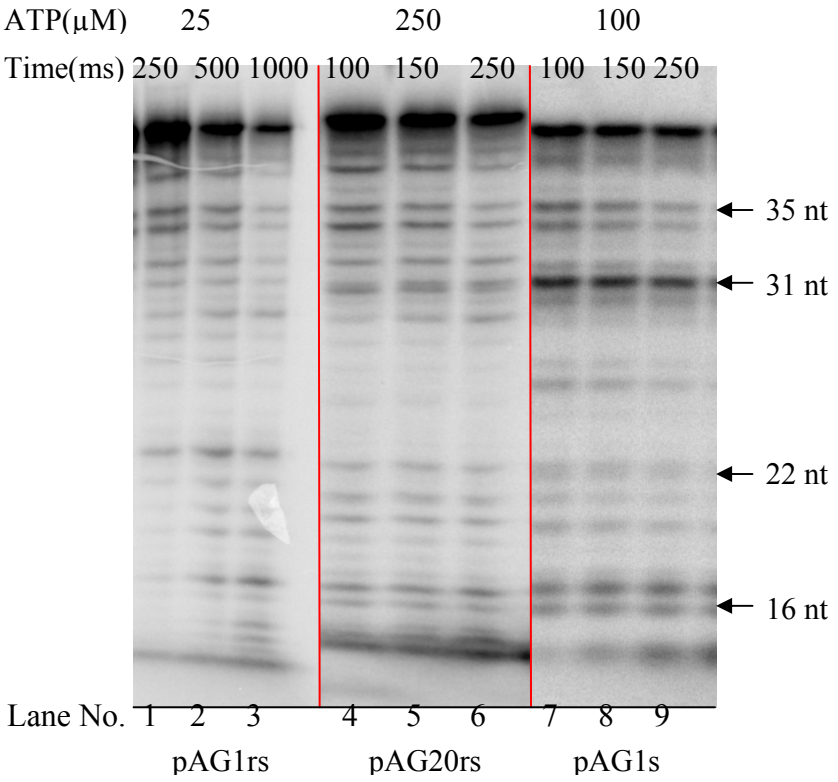

Fig. 14a: **Exonuclease reaction with oligomers of three different sequences.** Intermediates and products of the exonuclease reaction of RecBCD on 5' end labeled oligomers of the same length (40 nucleotides) but three different sequences (pAG1rs, pAG20rs and pAG1s) at 25μM, 250μM and 500μM ATP, respectively. Gel images are placed side by side to compare the positions of cleavages on these oligomers. Reactions were carried out at 25ºC in 25mM Tris-acetate (pH 7.5), 1mM DTT and 8mM Mg^{++}. The enzyme and the DNA concentrations were 160nM and 15.5nM respectively.

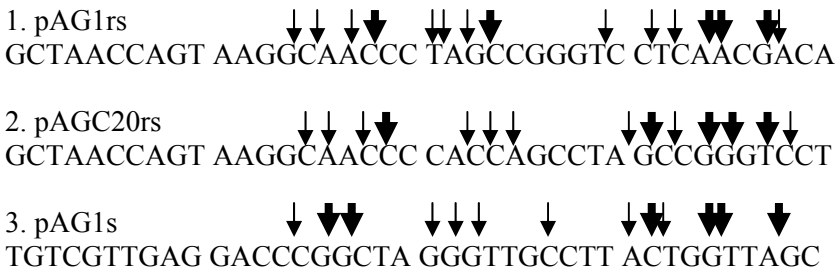

Fig. 14b: Positions of the major and the minor nucleolytic cleavages in three oligomer sequences.

nucleotide at the 3' end. Also, the enzyme does not cleave the DNA at every nucleotide; rather, a strong intermediate band appears each time after a gap of 2-3 nucleotides. This supports the finding that exonuclease function of RecBCD consists of short endonucleolytic cleavages [MacKay and Linn (1974), Muskavitch and Linn (1982)].

Second, the positions of nucleolytic cleavage are different for different sequences. This indicates that the enzyme selects the position of the cleavage depending on the nucleotide sequence at around the position (Fig. 14b). For example, the sequences around five main cleavages creating strong bands in the sequence pAG1rs are CG•AC, AA•CG, CA•AC, AG•CC and AC•CC. The sequences around six main cleavages in the sequence pAG1s are TA•GC, GG•TT, TG•GT, TA•CT, GG•CT and CG•GC. So far, we do not know the underlying basis of that selection.

Third, when the cleavage patterns of the three sequences were compared as shown in Fig. 14a, a similarity was found at some positions. Since some differences were also found, it could not be concluded that such cleavage pattern appeared due to some position dependent cleavages on the strand.

Exonuclease reaction of RecBCD with 3′-end labeled 40 nucleotide single-stranded oligomers:

RecBCD exonuclease reaction was also carried out with 3′ labeled single stranded oligomers. In all the reactions, both ends of the DNA substrate were free to bind to the enzyme. So far, we were able to see exonuclease reaction products with 5′-end labeled DNA strand, which indicated that exonuclease reaction can start from the 3′-end. This reaction was done to see if any exonuclease reaction can start from the 5′-end of the DNA, within the time range, 0 - 1 second.

From the studies of Chen et al. (1998) it was clear that the nuclease activity of RecBCD near the 5′-end is much less than that near the 3′-end. But, there was no study to find out the DNA intermediates of the exonuclease activity near the 5′-end. We wanted to find out if any significant amount of 5′-end nuclease product formed within the short time periods used in our other studies with 5′-end labeled DNA. We wanted to be sure that the potential DNA bands, those we observed in our studies with 5′-end labeled DNA, were from 3′-5′ exonuclease activity and not from 5′-3′ exonuclease activity.

Reactions were done with 32nM DNA and 400nM RecBCD, in the presence of 1mM ATP and 8mM Mg^{++}. DNA and enzyme were pre-incubated and ATP was added to start the reaction. We carried out exonuclease reactions at 100μM ATP for different time periods from 0 to 500 msecs and at different ATP concentrations (25μM, 250μM and 500μM ATP) for a fixed time period (200ms). We can see in the gel image (Fig. 15) that there are very faint bands on the upper part of the gel. These

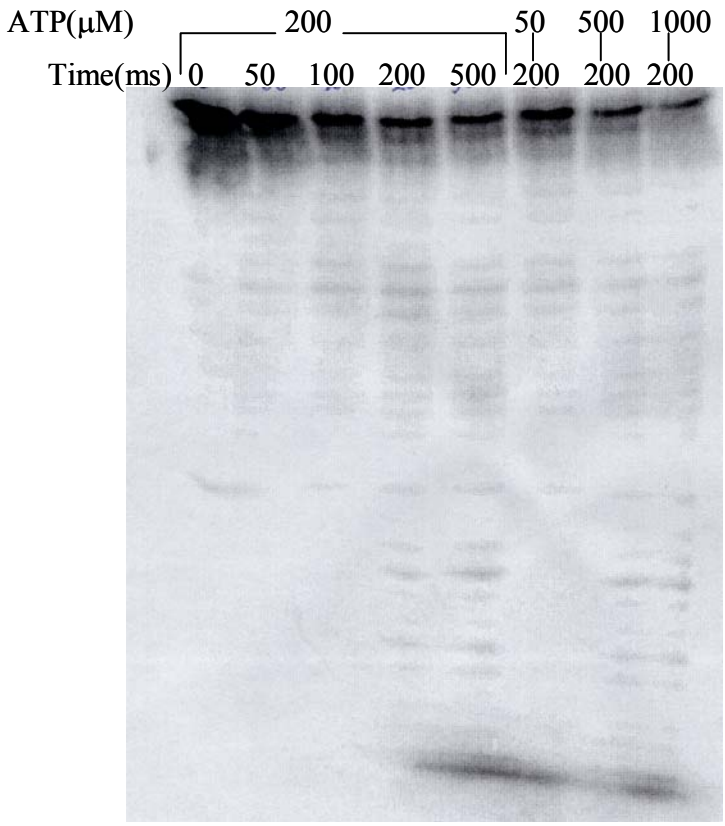

Fig. 15: Exonuclease reaction with a 3' labeled oligomer. Sequencing gel images of nuclease reactions of RecBCD with 3′ labeled oligomer pAG1s at 25ºC, in 25mM Tris-acetate (pH 7.5), 1mM DTT and 8mM Mg^{++}. The enzyme and the DNA concentrations were 160nM and 15.5nM respectively.

bands could be formed by nuclease reactions near the 5' end of the DNA. But there is no increase and decrease in band intensities with time and with the increase of the ATP concentration. This indicates that these bands were not formed by the nuclease activity of the enzyme molecules translocating from the 5' end towards the 3' end. Rather, they were present initially in the labeled DNA sample.

When we look at the lower part of the gel, however, we can see some stronger bands appearing with longer time points or with higher ATP concentrations. Since we cannot see similar reactions near the 5' end, we can conclude that these bands were formed by reactions from the 3' end. The very strong bands at the end of the gel indicate small 3' end labeled products formed due to nuclease activities near the 3' end. In conclusion we can say that there are no significant exonuclease reaction intermediates from cleavages near the 5' end formed with these substrates within our time range.

Exonuclease reaction of RecBCD with short single-stranded oligomers at different ATP concentrations, quantitation of products and analysis:

RecBCD was allowed to react with ssDNA oligomers for different time periods ranging from 0 to 2sec. Four different ATP concentrations were used, 10μM, 25μM, 100μM and 500μM. At each ATP concentration, reactions were carried out under two different conditions, in the presence of the unlabeled DNA trap or in the absence of any trap. Since we know that the enzyme cleaves a DNA strand in the 3'-5' direction more extensively than in the 5'-3' direction, we used 5' labeled substrates in most of our studies. As the enzyme moves along the DNA in the 3'-5' direction, cleaving the DNA in short steps, progressively shorter 5' labeled intermediates appear and disappear with time. The results are shown in Figures 16, 17, 18 and 19.

This experiment was done to study and compare the behavior of the enzyme at different ATP concentrations with single stranded DNA as substrates. RecBCD needs ATP for unwinding a double stranded DNA and also to move along a DNA strand. Change of unwinding rate with change of ATP concentration has been studied by other research groups [Lucius et al., (2004a)]. Here we have tried to find out the change of translocation rate at different ATP concentrations. This study has given us a chance to compare the behavior of the enzyme with two different kinds of DNA substrates, single stranded and double stranded.

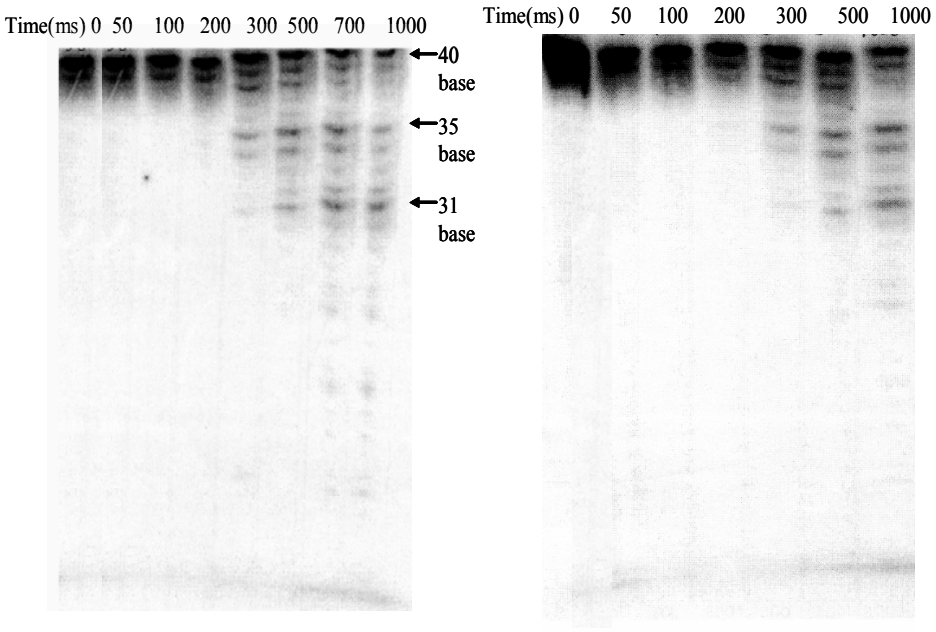

10μM ATP, without trap 10μM ATP, with trap

Fig. 16: Exonuclease reaction at 10μM ATP. Sequencing gel images of nuclease reactions of RecBCD with the oligomer pAG1s at 25ºC, in 25mM Tris-acetate (pH 7.5), 1mM DTT, 10μM ATP and 8mM Mg^{++}. The enzyme and the DNA concentrations were 160nM and 15.5nM respectively. Reactions were done in the presence and absence of 150 times more concentrated unlabeled DNA trap.

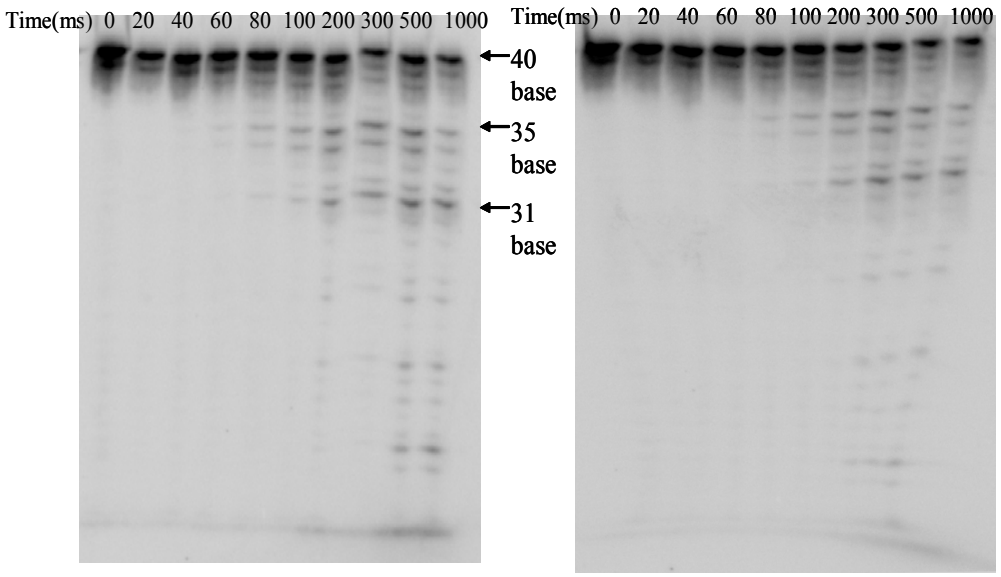

Fig. 17: Exonuclease reaction at 25μM ATP. Sequencing gel images of nuclease reactions of RecBCD with the oligomer pAG1s at 25ºC, in 25mM Tris-acetate (pH 7.5), 1mM DTT, 25μM ATP and 8mM Mg^{++}. The enzyme and the DNA concentrations were 160nM and 15.5nM respectively. Reactions were done in the presence and absence of 150 times more concentrated unlabeled DNA trap.

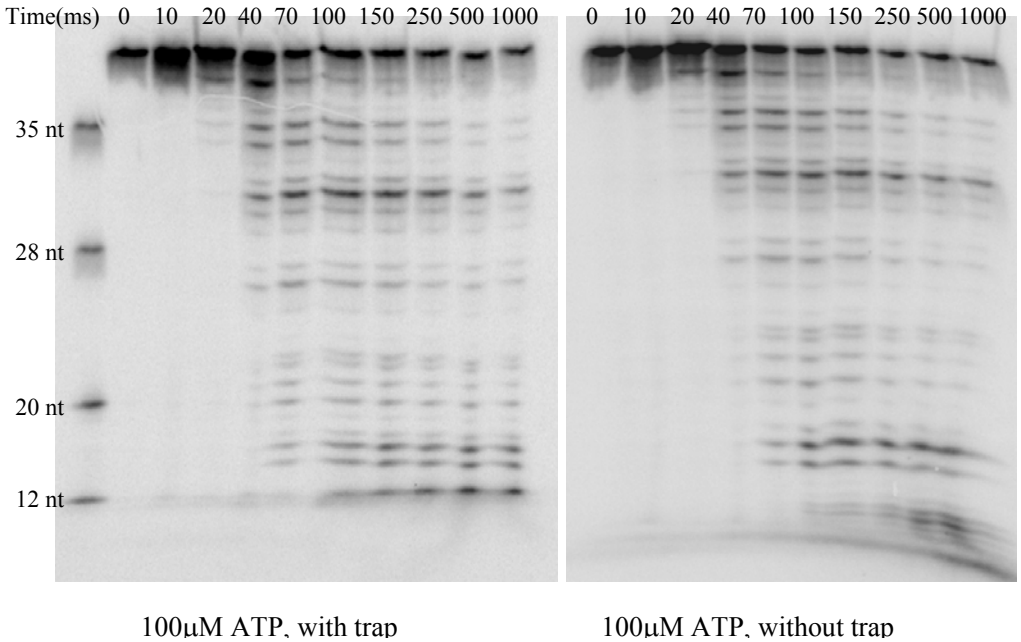

Fig. 18: Exonuclease reaction at 100μM ATP. Sequencing gel images of nuclease reactions of RecBCD with the oligomer pAG1s at 25ºC, in 25mM Tris-acetate (pH 7.5), 1mM DTT, 100μM ATP and 8mM Mg^{++}. The enzyme and the DNA concentrations were 160nM and 15.5nM respectively. Reactions were done in the presence and absence of 150 times more concentrated unlabeled DNA trap.

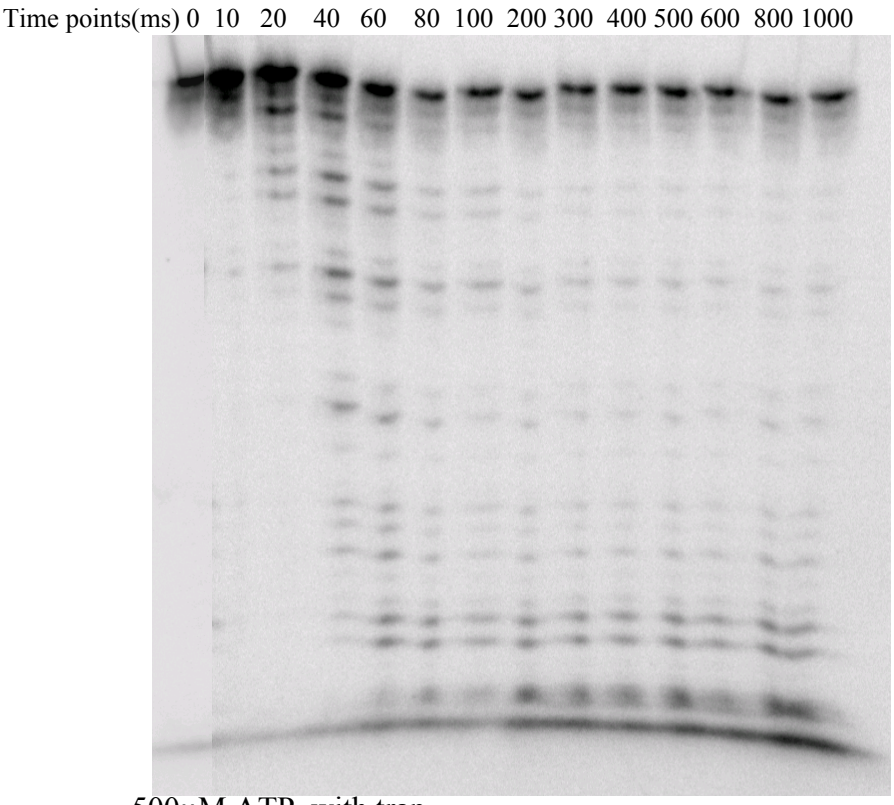

Fig. 19: Exonuclease reaction at 500μM ATP. Sequencing gel images of nuclease reactions of RecBCD with the oligomer pAG1s at 25ºC, in 25mM Tris-acetate (pH 7.5), 1mM DTT, 500μM ATP and 8mM Mg^{++}. Reactions were done in the presence of 100 times more concentrated unlabeled DNA trap.

By looking at the gel images, it can be seen that there is a lag time period after the reaction is started by addition of ATP and before the first nuclease reaction product appears. The lag time increases with decreasing ATP concentrations. But it remains unaffected by the presence or absence of a DNA trap at any particular ATP concentration.

It can also be seen that at any ATP concentration, some fraction of the substrate does not go into the nuclease reaction within the 1 second time period. In other experiments we allowed the reaction to continue for as long as 2 seconds, but still some amount of the 40 nucleotide substrate was left unreacted (results not shown).

This could be because of some enzyme molecules not being able to start the nuclease reaction on the bound DNA molecules. The enzyme – DNA complex could be inactive with respect to the nuclease reaction and be unable to undergo isomerization to the active complex. We also considered the possibility that some enzyme molecules are not strongly bound to the DNA and they dissociate and can reassociate again in absence of a trap.

In our experiments, we could see the number and relative amounts of the nuclease reaction products. There was not any change in the pattern and relative amounts of intermediates and products with the change of the ATP concentration. This pattern was found to be maintained at a still higher ATP concentration (500μM). This indicates that in the given reaction condition and within the given range of ATP concentration, the nuclease activity of the enzyme remains unaffected by the rate of translocation of the enzyme.

All the intermediates appear and disappear with time, except the 31mer intermediate, which appears and does not disappear. For some reason, nuclease activity of the enzyme on this DNA is inhibited. However, not all of the enzyme molecules are inhibited after the formation of the 31mer DNA, because we can see other intermediates smaller than the 31mer appearing and disappearing. One possibility could be that the enzyme simply dissociates from this intermediate for some sequence specific reason. Another possibility is that the enzyme remains bound and continues to move along the DNA, but the 3' end of the DNA is no longer accessible to the nuclease site.

It has been shown in the crystal structure of the enzyme [Singleton et al. (2004)] that the 3' end of the DNA can exit from its channel in the RecB subunit in two different directions (see Fig. 5). One exit leads to the nuclease domain of RecB. If the 3' end takes this exit, then it possibly comes in contact with the nuclease site and gets cleaved. The other exit bypasses the nuclease domain, and if the DNA end takes this exit then it cannot get cleaved by the enzyme anymore. The factors governing the choice of one channel over the other by the DNA is not known. In most cases the 3' end strand gets cleaved, which indicates that in general the DNA takes the exit towards the nuclease domain. However, for some unknown reason a fraction of the 31mer may take the alternate exit and may not get cleaved by the enzyme anymore.

We can think of another reason behind the inhibition of nuclease activity after the formation of the 31mer. There could be some sequence upstream to the 3' end of the 31mer which interacts strongly with some peptide sequence in RecBCD along the path through which the DNA has to move in order to reach to the nuclease active site.

Thus, the end part of the DNA might remain stuck to that particular sequence, while the enzyme can still move on along the DNA. In the introduction part, we have already discussed the *Chi* sequence, which is thought to have a similar effect. A few other sequences are also known to have *Chi* like effects [Cheng and Smith (1987)]. Similarly, some part of the 31mer DNA may be a new member of these *Chi* like sequences.

In our earlier experiments, we saw that using a very high concentration of DNA trap did not affect the nuclease activity of the enzyme on the DNA, which was already bound to it. Those experiments were done at 100μM ATP concentrations. In these experiments we used ATP concentrations as low as 25μM and 10μM, and still the effect of the DNA trap on the nuclease activity was negligible. This indicated that translocation of the enzyme on single stranded DNA was processive at these different ATP concentrations.

We quantitated the DNA substrate and intermediate and product bands. We selected the substrate, and three other main intermediates from each set of time points for kinetic analysis. Then we carried out simulations using mechanisms 2a and 2b (Fig. 22, Data analysis section) with the KinTekSim program, as described in the data analysis section. Fig. 20 is a graph showing the time courses of the 40mer substrate at different ATP concentrations. We can see that the rate of decrease of the 40mer substrate increases with increasing ATP concentration and the lag time increases with decreasing ATP concentration.

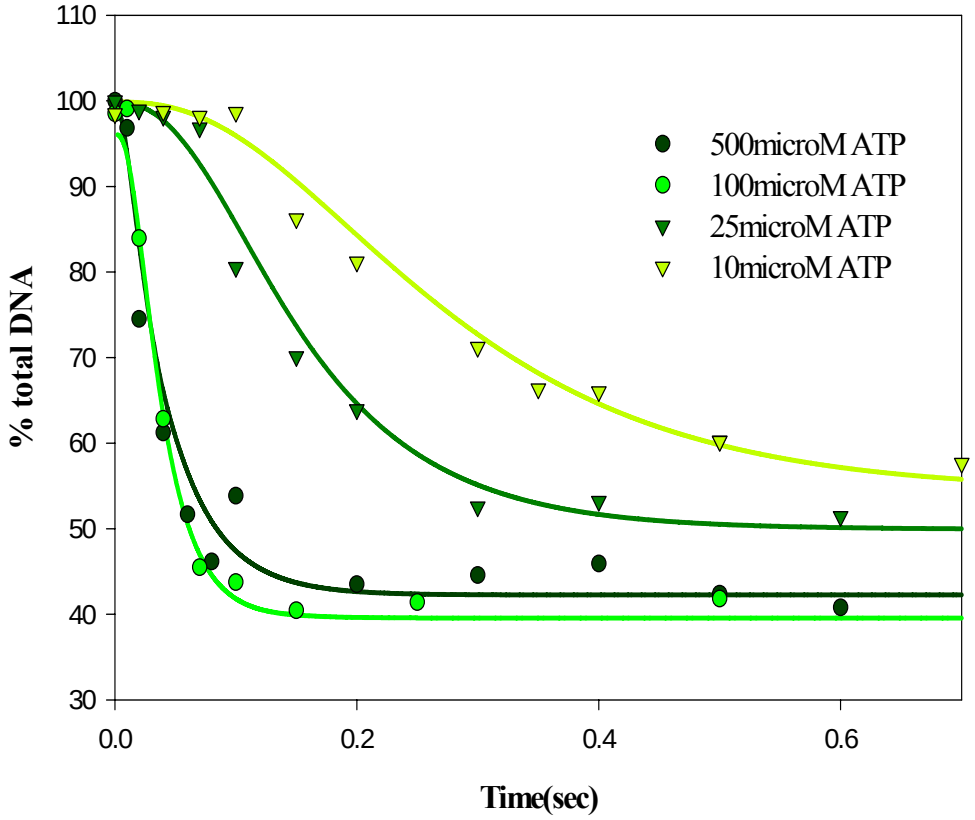

Fig. 20: Time course of the 40 nucleotide substrate at different ATP concentrations. Simulations were done by using Mechanism 2b as discussed in the data analysis section.

The final extent of reaction was not reproducible at the same reaction condition. It was found to vary to some extent, when the same experiment was repeated. In the above graph, the final plateau area of the 500μM and 100μM time courses indicate that 39% of the 40 nucleotide substrate remains unreacted at 100μM ATP, while 42% remains unreacted at 500μM ATP. However, it was found by data analysis of these two time courses, the rate of decrease of the substrate is higher at 500μM ATP than at 100μM ATP (See Table 10 in the data analysis section).

Exonuclease reaction of RecBCD with a 40 base oligomer without any pre-incubation:

We carried out an exonuclease reaction between RecBCD and the oligomer pAG1s, without any pre-incubation of the enzyme with the DNA. Radioactively labeled DNA substrate was added to reactant A, and RecBCD, mixed with 200μM ATP (100μM, final concentration) was included in reactant B. When both reactants are mixed in the reaction loop, the enzyme binds at the end of the DNA and then it starts moving along it and starts forming the nuclease cleavage products.

In our earlier experiments at the same ATP concentration, we pre-incubated the enzyme and the DNA. The enzyme had sufficient time to bind to the end of the DNA before reaction was started by the addition of ATP. Here, as the two reactants are mixed, the enzyme takes some time to bind to the DNA end and then it starts the translocation and nuclease activity. So, in this experiment, the enzyme is expected to have a longer lag time period than the experiment at 200μM ATP, with pre-incubation.

The result (Fig. 21) shows that this reaction causes a longer lag time period than the exonuclease reaction with the pre-incubation of the DNA and the enzyme, at the same ATP concentration. Also the extent of reaction is low, as in previous reactions. We quantitated the bands and collected the data for the 40-mer oligomer and the intermediates as described before. Then we used mechanism 3 to get the simulated graphs that overlaid on the data as discussed in the data analysis section.

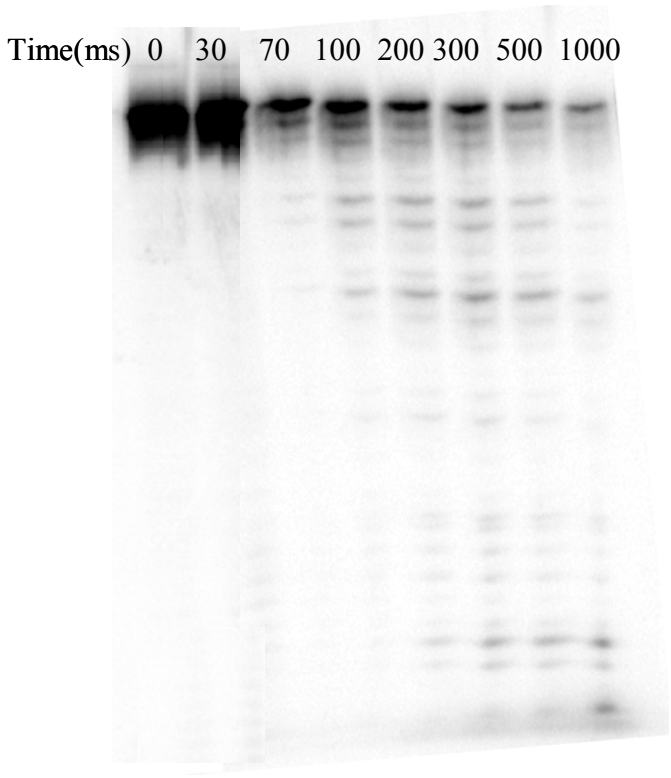

Fig. 21: Exonuclease reaction without the pre-incubation of the enzyme and the DNA. Sequencing gel images of nuclease reactions of RecBCD with the oligomer pAG1s at 25ºC, in 25mM Tris-acetate (pH 7.5), 1mM DTT, 100µM ATP and 8mM Mg^{++}. The enzyme and the DNA concentrations were 160nM and 15.5nM respectively. This reaction was done without the pre-incubation of the DNA and the enzyme. The enzyme was mixed with ATP and then DNA was added to start the reaction.

DATA ANALYSIS:

Mechanism of reaction:

In our experiments we mixed RecBCD with the DNA substrate and incubated it for a few minutes before starting the reaction by adding ATP. This was done to allow sufficient time for the enzyme to bind to the DNA ends. The enzyme was 10 times more concentrated than the DNA. It is known that RecBCD has high affinity for DNA ends (Gabbidon et al. 1998). We assumed that, before the reaction starts, every DNA molecule is bound to at least one enzyme molecule and that the concentration of the DNA-enzyme complex has the same concentration as the DNA.

Fig. 22 shows the mechanisms that we used to carry out the kinetic analysis of the data collected from the nuclease reactions. In these mechanisms, E represents the enzyme, D40 represents the 40mer DNA substrate, and E2D40, E1D40, E0D40 and ED40 designate four different complexes of the enzyme with the 40mer DNA substrate. E2D40, E1D40, and ED40 are three different forms of the active complex, while E0D40 is an inactive form of the complex. ED38, ED35 and ED31 represent the complexes of the enzyme with the 38mer, 35 and 34 mers and 31mer intermediates respectively.

Mechanism 1a:

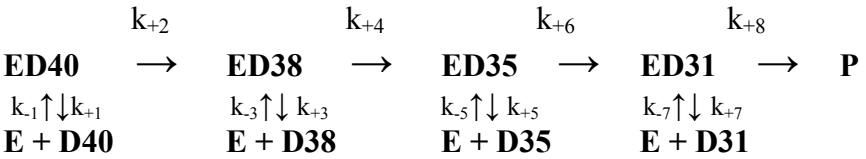

Mechanism 1b:

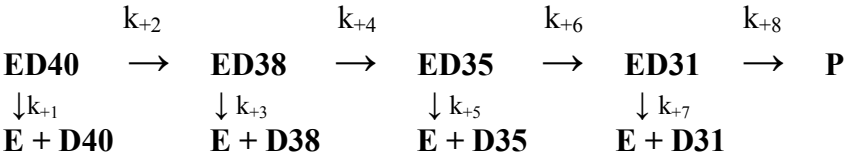

Mechanism 2a:

Mechanism 2b:

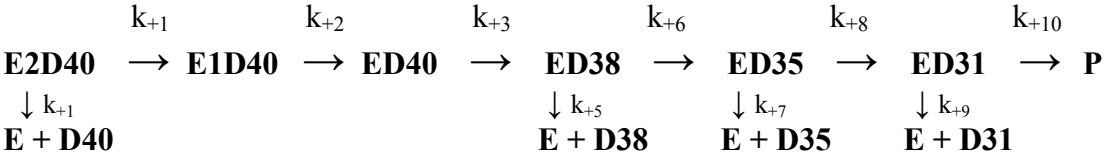

Mechanism 3:

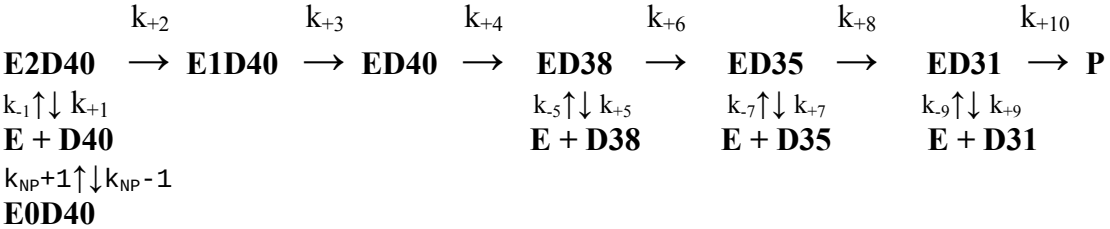

Fig. 22: Mechanisms used to model the reaction kinetics

In 1993 Dixon and Kowalczykowski showed that the 3' strand is cut much more extensively than the 5' strand by RecBCD. The work of Chen et al. (1998) showed that the major nuclease products that are formed during a reaction between RecBCD and single stranded DNA are those produced by cleavage near the 3' end. A minor nuclease activity occurs near the 5'-end. Our exonuclease studies with 3' labeled DNA substrates within the millisecond time scale also showed negligible nuclease activity near the 5'-end compared to the activity near the 3'-end (Fig. 15, result section). The single stranded oligonucleotides used in our experiments are labeled at the 5'-end, so we are only able to see the reaction intermediates originating from the 3' end bound to the enzyme. Some fraction of the oligonucleotides may bind to the 5' end binding site of the enzyme. Based on our present knowledge we assume that they are not subject to nuclease activity to any considerable amount.

By this pre-steady state kinetic study we have been able to observe the DNA intermediates along with the final products of the exonuclease reaction. It is known that the enzyme is very processive on double stranded DNA [Roman et al. (1992)]. But it is not very well known how it behaves on single stranded DNA substrates. Here we took into consideration the possibility that the enzyme can dissociate from and re-associate again to the substrate and each of the intermediates. In the presence of an unlabeled DNA trap the enzyme can not reassociate with the DNA once it has dissociated. Mechanisms 1b and 2b represent that particular case. Mechanisms 1a and 2a represent the reactions done in the absence of any trap. We assume that with each nuclease cleavage, the DNA is shortened by 2-4 nucleotides. These shortened DNA molecules remain complexed to the enzyme, and act as intermediates for subsequent

nuclease activity. In our reaction mechanisms, we have represented each nucleolytic cleavage as a single step, where one enzyme–DNA complex is transformed into another enzyme-DNA complex.

In Mechanisms 1a and 1b, the enzyme and the DNA combine to form a complex ED40 when the enzyme and the DNA are pre-incubated. When the reaction is started by the addition of ATP, a fraction of ED40 dissociates reversibly (Mechanism 1a) or irreversibly (in the presence of DNA trap, Mechanism 1b) to form free enzyme and DNA. The rest of the ED40 molecules undergo nuclease cleavage forming ED38. ED38 then gets cleaved forming ED35 and ED34. Both of these complexes then undergo nucleolytic cleavages forming ED31, which then forms other downstream products. Bands 35 and 34 differ in length only by one nucleotide. They were found to have similar values in all the time points. So we assumed that they were formed during the same cleavage reaction. We added their values and considered it as the value of the single band, 35mer.

E2D40 and E1D40 are two other conformations of the ED40 complex. These two complexes appear in Mechanism 2a, 2b and 3. We included two extra steps in Mechanism 2a and 2b. In these two schemes, E2D40 is the complex that is formed during the pre-incubation. When the reaction starts, some E2D40 molecules may dissociate reversibly (Mechanism 2a) or irreversibly (Mechanism 2b) to form free enzyme and DNA. The rest of E2D40 changes conformation to form E1D40, which again changes conformation to ED40, which then undergoes nuclease cleavage forming ED38.

Mechanism 3 represents the reaction where the enzyme and the DNA are not pre-incubated. The reaction is started by mixing one with the other. In this case free enzyme and DNA combine irreversibly to form E0D40, an inactive form of the complex of the enzyme with the 40mer substrate. The enzyme and the DNA also combine reversibly to form E2D40, which then changes to E1D40, ED40 and so on.

Simulations:

Simulations were done using the simulation program (Kinsim) of the Kinteksim software version 3.20, provided by KinTek Corporation. We also tried to use the non-linear least squares fitting program (Fitsim) in Kinteksim to fit the data. Each mechanism shown in Fig. 22 was tested with each data set. For any mechanism, we imparted some value to the rate constants and then checked how well the simulated graph overlaid on a particular set of data. Then we tried to use Fitsim to get the fitted values by floating all the rate constants. We got better superimposition for some parts of the data from the reactions done in the presence of 100μM and 500μM ATP. The errors for the rate constants for the nuclease steps were 25-50% of the rate constant itself and the errors for the dissociation steps were 100% of the rate constant or larger.

Then we changed the values of the rate constants one at a time and used Kinsim to see if the superimposition with the data becomes better with that change. Finally, we settled upon one set of rate constant values which, we thought, overlaid best on that particular set of data. After the final simulation step we did some small adjustments of the values of some rate constant values by using Fitsim and floating only one rate constant or a couple of rate constants at a time.

We could not use Fitsim for the data from the reactions done in the presence of 10μM and 25μM ATP. The program did not run with mechanisms 1a and 1b. With mechanisms 2a and 2b the fitted graph did not overlay on all parts of the data. The values of the rate constants were unreasonably large. So, we mainly carried out simulations with Kinsim to find the graphs which seemed to overlay best on the data points.

From each reaction, we took the data points of the time courses of the 40mer substrate and the 38mer, 35mer and 31mer products and plotted them on a single graph. Then we used the program to get a simulated graph for each of the time courses. Finally we made changes and small adjustments to the values so that all four simulated graphs can be overlaid on the corresponding data points at the same time.

Initially we wanted to use the simplest kinetic mechanism for our data. We first tried to use Mechanism 1a and Mechanism 1b for the simulation. We could place the simulated graph over the data of the exonuclease reactions at 100μM ATP. Fig. 23 and Fig. 24 are the graphs obtained by carrying out the simulations using Mechanism 1a and 1b. The corresponding rate constant values are shown in Table 5.

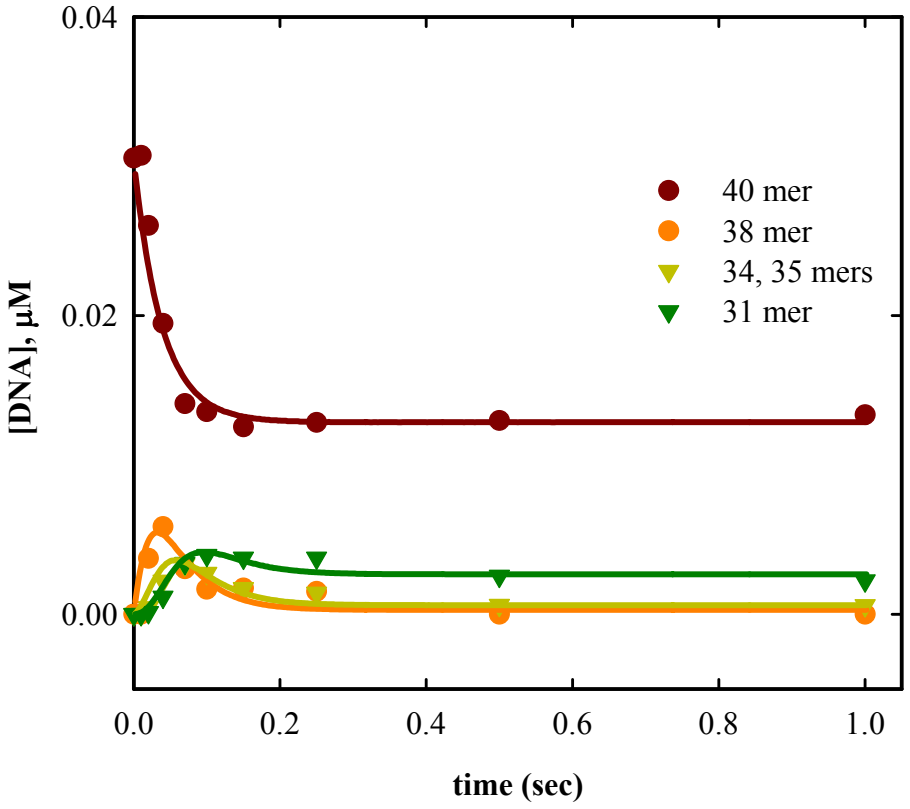

Fig. 23: DNA concentration vs. reaction time plot for the exonuclease reaction at 100µM ATP simulated by using Mechanism 1b. Time courses of the 40mer substrate and the 38mer, 35, 34mers and 31mer intermediates resulting from the nuclease reaction of RecBCD with the oligomer pAG1s at 25ºC, in 25mM Tris-acetate (pH 7.5), 1mM DTT, 100µM ATP and 8mM Mg^{++} (see Fig.18, Results section). The enzyme and the DNA concentrations were 320nM and 31nM respectively. The reactions were done in the presence of 150 times more concentrated unlabeled DNA trap. Graphs were simulated by using Mechanism 1b.

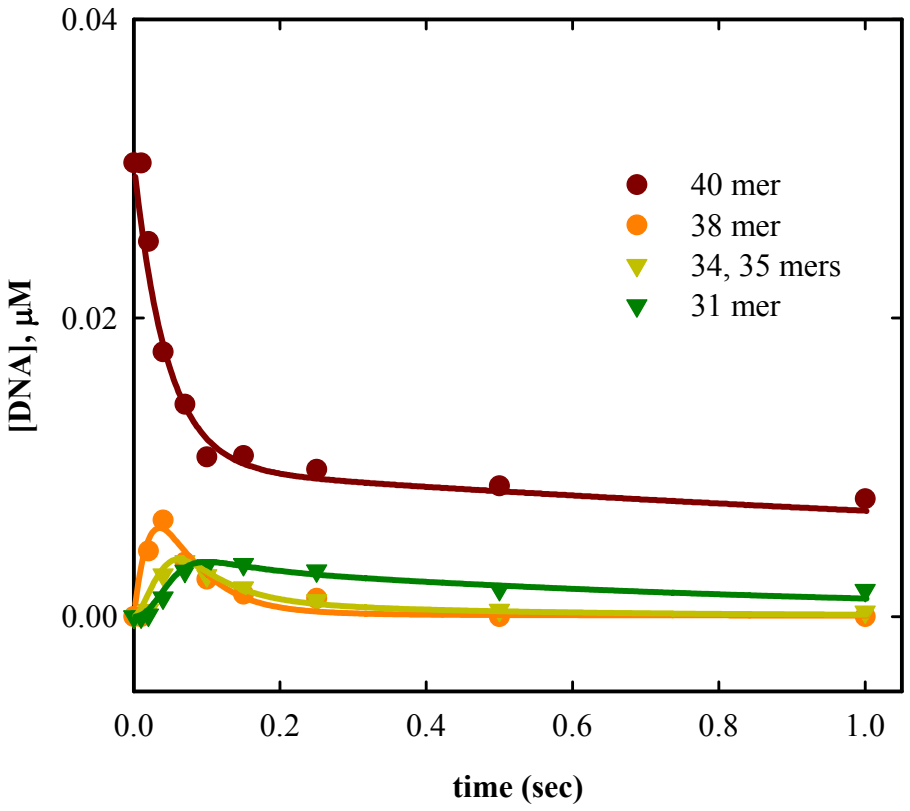

Fig. 24: DNA concentration vs. reaction time plot for the exonuclease reaction at 100µM ATP simulated by using Mechanism 1a. Time courses of the 40mer substrate and the 38mer, 35, 34mers and 31mer intermediates resulting from the nuclease reaction of RecBCD with the oligomer pAG1s at 25ºC, in 25mM Tris-acetate (pH 7.5), 1mM DTT, 100µM ATP and 8mM Mg^{++} (see Fig.18, Results section). The enzyme and the DNA concentrations were 320nM and 31nM respectively. The reactions were done in the absence of any DNA trap. Graphs were simulated by using Mechanism 1a.

Rate constant	100μM ATP Without trap	100μM ATP With trap
k_{+1} (s^{-1})	7	11
k_{-1} ($\mu M^{-1}s^{-1}$)	2	N.A.
k_{+2} (s^{-1})	15	15
k_{+3} (s^{-1})	0.7	0.6
k_{-3} ($\mu M^{-1}s^{-1}$)	33	N.A.
k_{+4} (s^{-1})	36	36
k_{+5} (s^{-1})	2.6	1.7
k_{-5} ($\mu M^{-1}s^{-1}$)	14	N.A.
k_{+6} (s^{-1})	50	46
k_{+7} (s^{-1})	11	7
k_{-7} ($\mu M^{-1}s^{-1}$)	7	N.A.
k_{+8} (s^{-1})	59	38

Table 5: **Rate constant values obtained by simulation of the nuclease reactions at 100μM ATP by using mechanisms 1a (shown below, for the reaction without trap) and 1b (for the reactions with trap).** [N. A. – The step is not relevant due to the trap.]

Mechanism 1a:

$$\underset{\mathbf{E+D40}}{\overset{k_{-1}\uparrow\downarrow k_{+1}}{\mathbf{ED40}}} \xrightarrow{k_{+2}} \underset{\mathbf{E+D38}}{\overset{k_{-3}\uparrow\downarrow k_{+3}}{\mathbf{ED38}}} \xrightarrow{k_{+4}} \underset{\mathbf{E+D35}}{\overset{k_{-5}\uparrow\downarrow k_{+5}}{\mathbf{ED35}}} \xrightarrow{k_{+6}} \underset{\mathbf{E+D31}}{\overset{k_{-7}\uparrow\downarrow k_{+7}}{\mathbf{ED31}}} \xrightarrow{k_{+8}} \mathbf{P}$$

It can be seen in Fig. 24 that the time course of the 40mer substrate has two phases. The first phase, when almost 65% of the substrate goes into the nuclease reaction, is followed by a much slower second phase. These data represent the experiment where we did not use any unlabeled DNA trap. The slow second phase may arise due to the slow isomerization of the inactive DNA enzyme complex to the active form. It can also arise if, during the first phase, some bound enzyme molecules dissociate from the DNA, reassociate slowly and start the nuclease reaction.

In Fig. 25, the time course of the 40mer substrate shows a fast initial phase and a second phase, where the plot forms a plateau horizontal to the x-axis. This means that in this case the reaction stops after the fast phase. In this experiment, we included excess unlabeled DNA trap, which can prevent any enzyme molecule from re-binding to the DNA. The absence of the slow second phase could be due to the inability of the free enzyme to bind the DNA in the presence of the trap. This also proves that the slow phase is not due to isomerization of an inactive enzyme-DNA complex to the active phase.

There is a lag time as small as 10 msec in the data points from these experiments, but there is no lag phase in the fitted graphs using mechanisms 1a and 1b. So the graph is not superimposed on that particular data point. Time courses of the 38mer, 35mer and 31mer intermediates sequentially appear and disappear. A small lag time can be seen in the time course of the 31mer intermediate. According to our mechanisms, the enzyme has to move along the DNA and make the 38mer and 35mer intermediates before it can reach to the position where it makes the nuclease

cut corresponding to the 31mer. We believe that this translocation time creates the lag time period.

The graphs simulated by using Mechanisms 1a and 1b did not overlay very well on the data of the reactions done in the presence of 25μM and 10μM ATP. We saw a lag time period as long as 70 msec and 100 msec in the case of the lower ATP concentrations, before any DNA intermediate starts appearing. So we included one extra step, with one extra DNA-enzyme complex, to account for the lag time period that can be seen in the gel pictures. Still the simulated graph did not overlay on the data around the lag phase very well. Then, we included two extra steps with two extra DNA-enzyme complexes (E2D40 and E1D40, shown in Mechanisms 2a and 2b), which resulted in a satisfactory superimposition.

Fig. 25 shows the simulated graphs of the 40mer substrate, for a reaction done in the presence of 10μM ATP, obtained by using zero, one or two extra steps before the first cleavage step. We can see that the time course of the 40mer substrate consists of three phases, a lag phase, a fast phase and a plateau phase. The graphs were simulated in such a way that all three of them overlaid fairly well on the data points. However, the best superimposition on the data points, representing the lag time, was attained with the graph simulated with two extra steps in the mechanism. The change from one phase to the other became clearer when we changed from no extra step to one extra step and then to two extra steps.

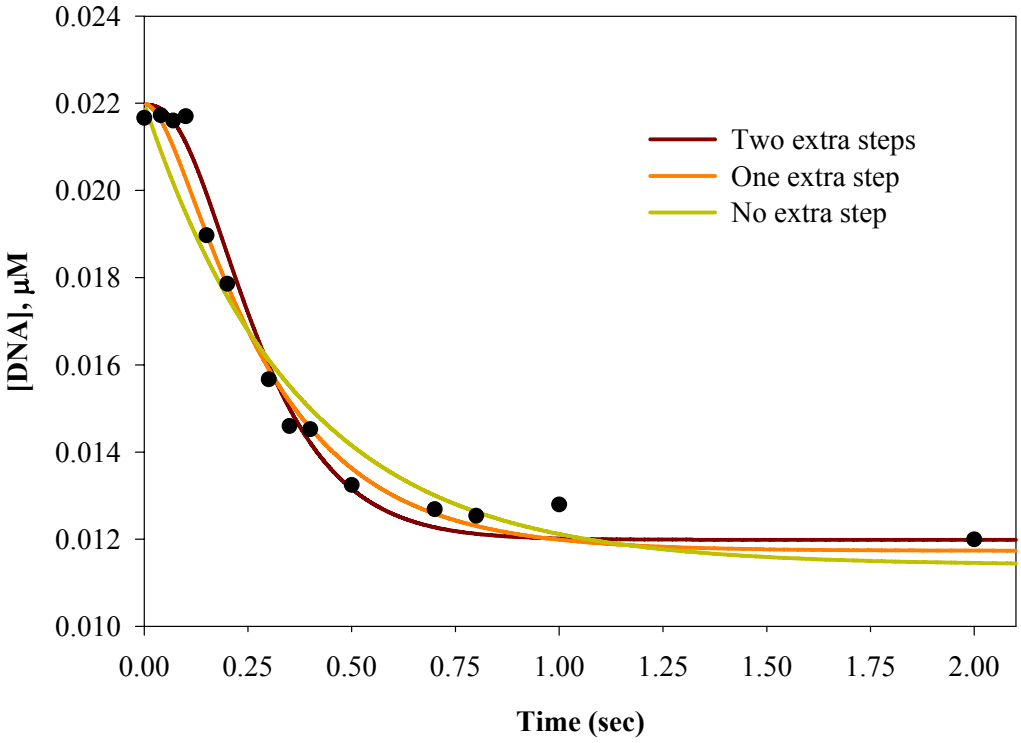

Fig. 25: The simulated graphs of the 40mer substrate using different mechanisms. The exonuclease reaction was done in the presence of 10µM ATP. The simulated graphs were obtained by using zero (Mechanism 1b) or one or two (Mechanism 2b) extra steps before the first cleavage step.

We tried to keep the values of the rate constants of the first four steps (k_{+1}, k_{-1}, k_{+2}, k_{+3}, k_{+4}) of Mechanisms 2a and 2b as low as possible for each data set. We found there is a minimum value of these constants, below which the simulated graph could not be superimposed on the data. The value of k_{+3} could then be increased to any extent without any effect on the graph. Anyway, we chose to keep the minimum value. The values of k_{+1} and k_{+2} affected the position of the plateau shaped end part of the time course of the 40mer substrate. The values of k_{+3} and k_{+4} had more to do with the initial lag time and the slope of the time course. k_{-1} controlled the slope of the end plateau.

We also showed the time courses of the 38base, 34base, and 31base intermediates. The values of k_{+1}, k_{+2}, k_{+3} and k_{+4} have some effect on the first part of the graphs including the lag time of each of the intermediates. The rest of the graph was then simulated by adjusting the values of the rate constants k_{+6}, k_{+8} and k_{+10} and dissociation constants k_{+5}, k_{+7} and k_{+9} to get the best superimposition.

Fig. 26 and Fig. 27 show the graphs for the data of exonuclease reactions done in the presence of 10μM) and 25μM) ATP concentrations by simulation, using Mechanism 2b. The values of the rate constants obtained by analyzing the data from the reactions done at 10μM ATP are shown in Table 6. Rate constants for the reaction done at 25μM ATP are shown in Table 7.

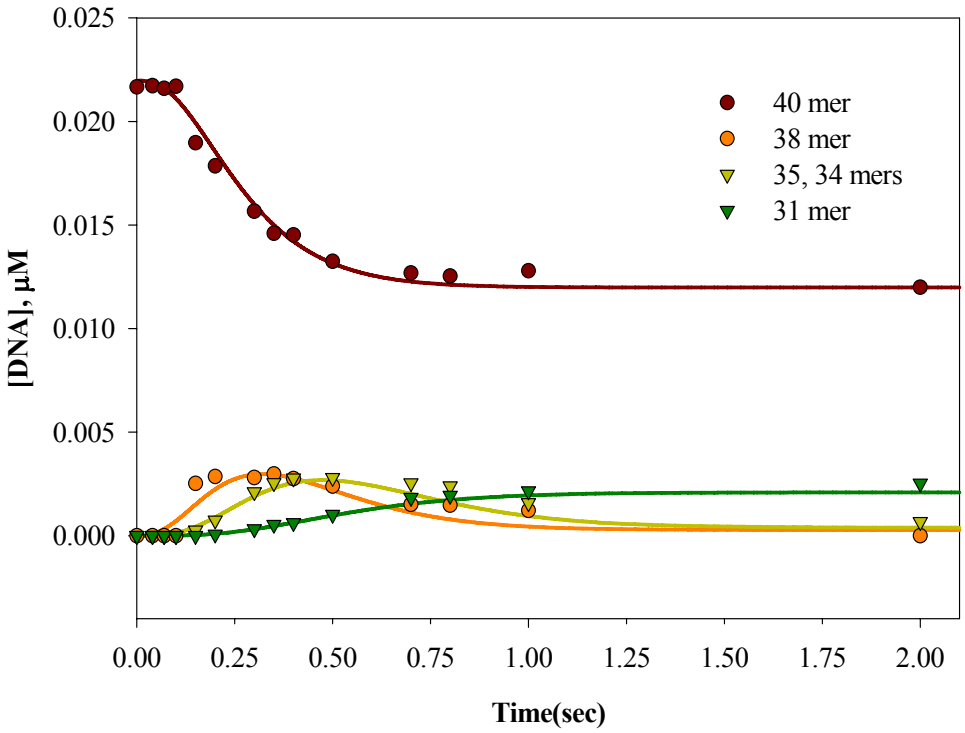

Fig. 26: DNA concentration vs. reaction time plot for the exonuclease reaction at 10µM ATP. Time courses of the 40mer substrate and the 38mer, 35, 34mers and 31mer intermediates resulting from the nuclease reaction of RecBCD with the oligomer pAG1s at 25ºC, in 25mM Tris-acetate (pH 7.5), 1mM DTT, 10µM ATP and 8mM Mg^{++} (see Fig.16, Results section). The enzyme and the DNA concentrations were 175nM and 22nM respectively. The reactions were done in the presence of 100 times more concentrated unlabeled DNA trap. The graph was simulated by using Mechanism 2b.

Rate constants	10μM ATP Without trap	10μM ATP With trap(1)	10μM ATP With trap(2)	Av. rate for each step (steps/sec) (± std. dev.)
k_{+1} (s^{-1})	4	5	6	5 (± 1)
k_{-1} ($\mu M^{-1}s^{-1}$)	1	N.A.	N.A.	N.A.
k_{+2} (s^{-1})	3	3	5	4 (± 1)
k_{+3} (s^{-1})	11	12	13	12 (± 1)
k_{+4} (s^{-1})	8	8	8	8 (± 0)
k_{+5} (s^{-1})	0	1	0.2	0.4 (± 0.5)
k_{-5} ($\mu M^{-1}s^{-1}$)	0	N.A.	N.A.	N.A.
k_{+6} (s^{-1})	6	5	7	6 (± 1)
k_{+7} (s^{-1})	0	2	0.25	1 (± 1)
k_{-7} ($\mu M^{-1}s^{-1}$)	0	N.A.	N.A.	N.A.
k_{+8} (s^{-1})	7.5	9	6	8 (± 2)
k_{+9} (s^{-1})	13	5	29	16 (± 12)
k_{-9} ($\mu M^{-1}s^{-1}$)	0	N.A.	N.A.	N.A.
k_{+10} (s^{-1})	34	20	100	51 (± 43)

Table 6: **Rate constant values obtained by simulation of the nuclease reaction at 10μM ATP by using mechanisms 2a (shown below, for the reaction without trap) and 2b (for the reactions with trap).** [N.A. – The step is not relevant due to the trap.]

Mechanism 2a:

$$\underset{}{\mathbf{E2D40}} \xrightarrow{k_{+2}} \mathbf{E1D40} \xrightarrow{k_{+3}} \mathbf{ED40} \xrightarrow{k_{+4}} \mathbf{ED38} \xrightarrow{k_{+6}} \mathbf{ED35} \xrightarrow{k_{+8}} \mathbf{ED31} \xrightarrow{k_{+10}} \mathbf{P}$$

$$k_{-1}\uparrow\downarrow k_{+1} \qquad k_{-5}\uparrow\downarrow k_{+5} \qquad k_{-7}\uparrow\downarrow k_{+7} \qquad k_{-9}\uparrow\downarrow k_{+9}$$

$$\mathbf{E + D40} \qquad \mathbf{E + D38} \qquad \mathbf{E + D35} \qquad \mathbf{E + D31}$$

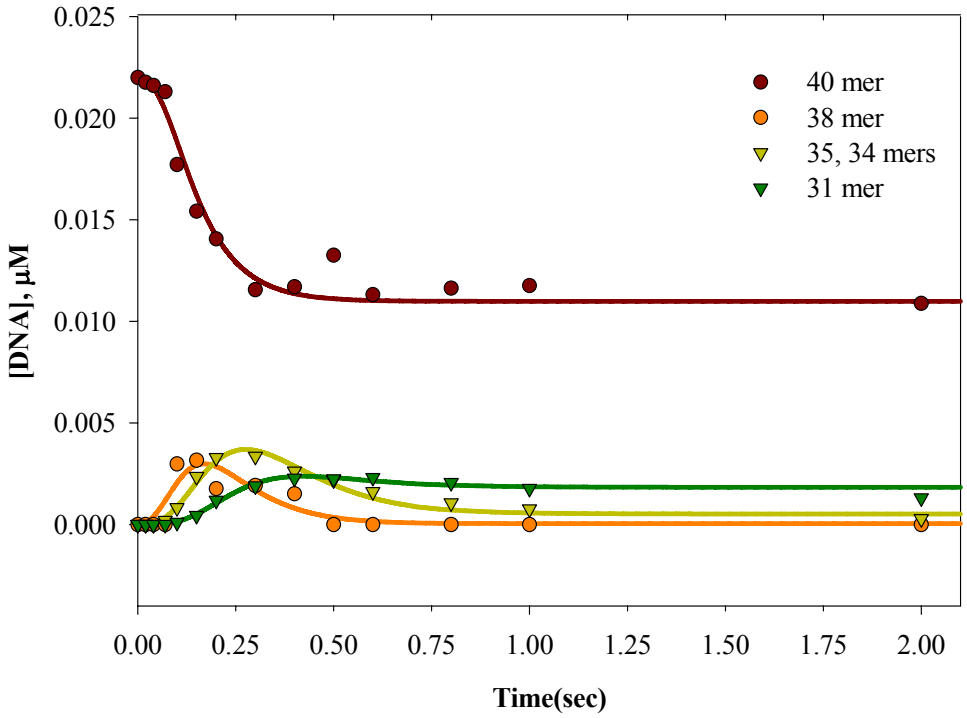

Fig. 27: DNA concentration vs. reaction time plot for the exonuclease reaction at 25µM ATP. Time courses of the 40mer substrate and the 38mer, 35, 34mers and 31mer intermediates resulting from the nuclease reaction of RecBCD with the oligomer pAG1s at 25ºC, in 25mM Tris-acetate (pH 7.5), 1mM DTT, 25µM ATP and 8mM Mg^{++} (see Fig.17, result section). The enzyme and the DNA concentrations were 175nM and 22nM respectively. The reactions were done in the presence of 100 times more concentrated unlabeled DNA trap. The graph was simulated by using Mechanism 2b.

Rate constants	25μM ATP Without trap	25μM ATP With trap	25μM ATP With trap	Av. rate for step (steps/sec) (± std. dev.)
k_{+1} (s^{-1})	7	11	6	8 (± 3)
k_{-1} ($\mu M^{-1}s^{-1}$)	0	N.A.	N.A.	N.A.
k_{+2} (s^{-1})	4	6	6	5 (± 1)
k_{+3} (s^{-1})	35	40	30	35 (± 5)
k_{+4} (s^{-1})	50	20	20	30 (± 17)
k_{+5} (s^{-1})	0.6	0.1	0.06	0.25 (± 0.3)
k_{-5} ($\mu M^{-1}s^{-1}$)	0	N.A.	N.A.	N.A.
k_{+6} (s^{-1})	9	7	14	10 (± 4)
k_{+7} (s^{-1})	0.4	0.6	0.4	0.5 (± 0.1)
k_{-7} ($\mu M^{-1}s^{-1}$)	0	N.A.	N.A.	N.A.
k_{+8} (s^{-1})	6	6	8	7 (± 1)
k_{+9} (s^{-1})	7	3	3	4 (± 2)
k_{-9} ($\mu M^{-1}s^{-1}$)	0	N.A.	N.A.	N.A.
k_{+10} (s^{-1})	20	14	14	16 (± 4)

Table 7: **Rate constant values obtained by simulation of the nuclease reaction at 25μM ATP by using mechanisms 2a (shown below, for the reaction without trap) and 2b (for the reactions with trap).** [N.A. – The step is not relevant due to the trap.]

Mechanism 2a:

$$\underset{}{\overset{k_{+2}}{\mathbf{E2D40}} \rightarrow \mathbf{E1D40}} \overset{k_{+3}}{\rightarrow} \mathbf{ED40} \overset{k_{+4}}{\rightarrow} \mathbf{ED38} \overset{k_{+6}}{\rightarrow} \mathbf{ED35} \overset{k_{+8}}{\rightarrow} \mathbf{ED31} \overset{k_{+10}}{\rightarrow} \mathbf{P}$$

$$\underset{\mathbf{E + D40}}{k_{-1}\uparrow\downarrow k_{+1}} \qquad \underset{\mathbf{E + D38}}{k_{-5}\uparrow\downarrow k_{+5}} \qquad \underset{\mathbf{E + D35}}{k_{-7}\uparrow\downarrow k_{+7}} \qquad \underset{\mathbf{E + D31}}{k_{-9}\uparrow\downarrow k_{+9}}$$

In the reaction done in the presence of 100μM ATP, a very small lag time could be seen, which could be ignored in the initial simulations. But later we used Mechanisms 2a and 2b to simulate the graph. That way we could include the lag period. Also by using Mechanism 2 instead of Mechanism 1 the value of the rate constants at each step increased.

Figures 28 and 29 show the graphs obtained by simulating the graphs for exonuclease reactions done in the presence of 100μM ATP, and 500μM ATP concentrations to Mechanism 2b. The values of the rate constants obtained by analyzing the data from the exonuclease reactions done at 100μM ATP are shown in Table 8. The rate constants for the reaction done at 500μM ATP are shown in Table 10.

Fig. 30 shows the time courses of the 31mer intermediate, simulated with the rate constant values obtained from the experiments done at different ATP concentrations. Each experiment was repeated three times at each ATP concentration, twice in the presence of unlabeled DNA trap and once in the absence of any trap.

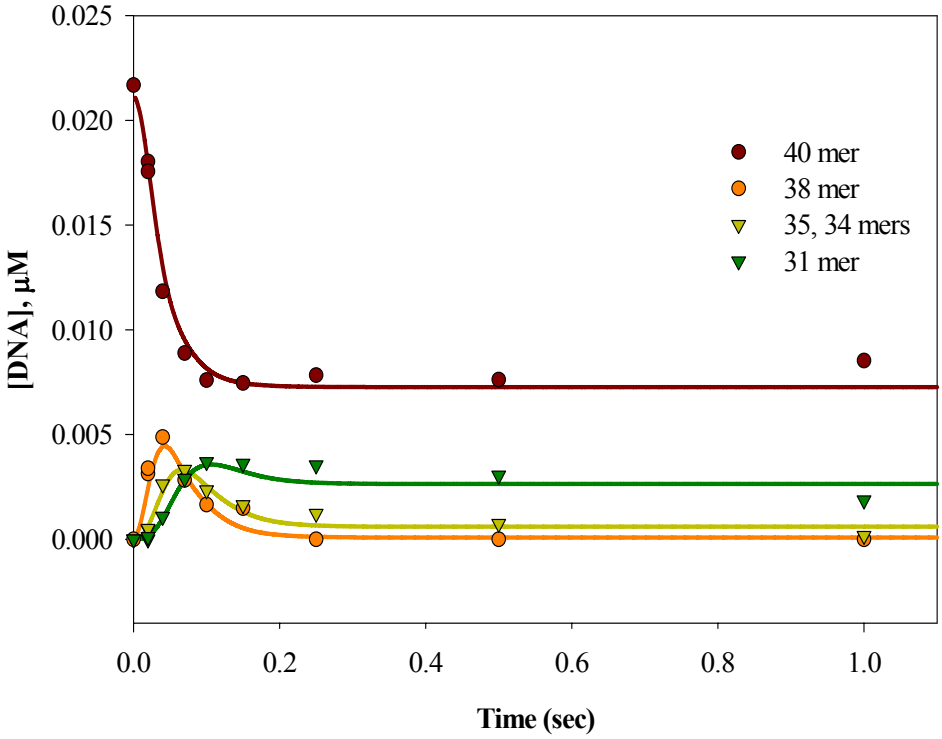

Fig. 28: DNA concentration vs. reaction time plot for the exonuclease reaction at 100µM ATP. Time courses of the 40mer substrate and the 38mer, 35, 34mers and 31mer intermediates resulting from the nuclease reaction of RecBCD with the oligomer pAG1s at 25ºC, in 25mM Tris-acetate (pH 7.5), 1mM DTT, 100µM ATP and 8mM Mg^{++} (see Fig.18, result section). The enzyme and the DNA concentrations were 175nM and 22nM respectively. The reactions were done in the presence of 150 times more concentrated unlabeled DNA trap. The graph was simulated by using Mechanism 2b.

Rate constants	100μM ATP Without trap	100μM ATP With trap	100μM ATP With trap	Av. rate for each step (steps/sec) (± std. dev.)
k_{+1} (s^{-1})	11	17.5	11	13.2 (± 3.8)
k_{-1} ($\mu M^{-1}s^{-1}$)	1	N.A.	N.A.	N.A.
k_{+2} (s^{-1})	23	24	21	23 (± 2)
k_{+3} (s^{-1})	160	161	160	160 (± 1)
k_{+4} (s^{-1})	166	166	182	171 (± 9)
k_{+5} (s^{-1})	0.7	0.7	0.25	0.6 (± 0.3)
k_{-5} ($\mu M^{-1}s^{-1}$)	0	N.A.	N.A.	N.A.
k_{+6} (s^{-1})	50	40	40	43 (± 6)
k_{+7} (s^{-1})	2	4	2	3 (± 1)
k_{-7} ($\mu M^{-1}s^{-1}$)	0	N.A.	N.A.	N.A.
k_{+8} (s^{-1})	65	70	44	60 (± 14)
k_{+9} (s^{-1})	11	11	10	11 (± 1)
k_{-9} ($\mu M^{-1}s^{-1}$)	3	N.A.	N.A.	N.A.
k_{+10} (s^{-1})	75	59	40	58 (± 18)

Table 8: **Rate constant values obtained by simulation of the nuclease reaction at 100μM ATP by using mechanism 2a (shown below, for the reaction without trap) and 2b (for the reactions with trap).** [N.A. – The step is not relevant due to the trap.]

Mechanism 2a:

$$\underset{k_{+1}\uparrow\downarrow k_{-1}}{\mathbf{E + D40}} \quad \overset{k_{+2}}{\longrightarrow} \quad \mathbf{E1D40} \quad \overset{k_{+3}}{\longrightarrow} \quad \mathbf{ED40} \quad \overset{k_{+4}}{\longrightarrow} \quad \underset{k_{+5}\uparrow\downarrow k_{-5}}{\mathbf{ED38}} \quad \overset{k_{+6}}{\longrightarrow} \quad \underset{k_{+7}\uparrow\downarrow k_{-7}}{\mathbf{ED35}} \quad \overset{k_{+8}}{\longrightarrow} \quad \underset{k_{+9}\uparrow\downarrow k_{-9}}{\mathbf{ED31}} \quad \overset{k_{+10}}{\longrightarrow} \quad \mathbf{P}$$

$$\mathbf{E + D40} \qquad\qquad \mathbf{E + D38} \qquad \mathbf{E + D35} \qquad \mathbf{E + D31}$$

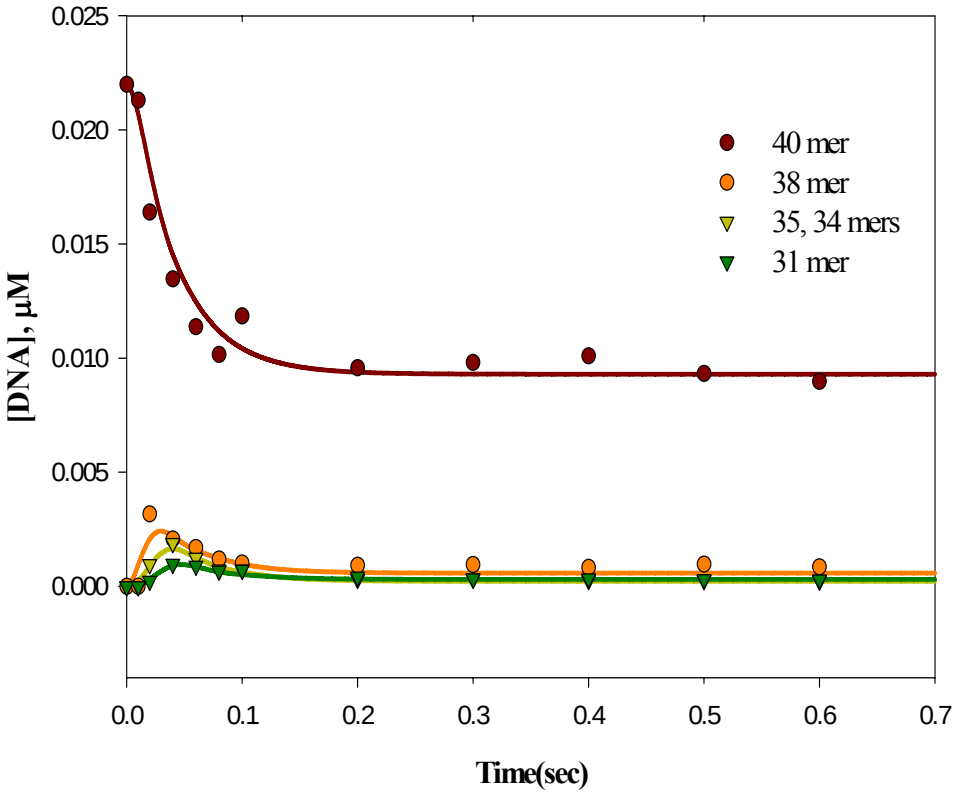

Fig. 29: DNA concentration vs. reaction time plot for the exonuclease reaction at 500µM ATP. Time courses of the 40mer substrate and the 38mer, 35, 34mers and 31mer intermediates resulting from the nuclease reaction of RecBCD with the oligomer pAG1s at 25ºC, in 25mM Tris-acetate (pH 7.5), 1mM DTT, 500µM ATP and 8mM Mg^{++} (Fig. 19, Results section). The enzyme and the DNA concentrations were 175nM and 22nM respectively. The reactions were done in the presence of 100 times more concentrated unlabeled DNA trap. The graph was simulated by using Mechanism 2b.

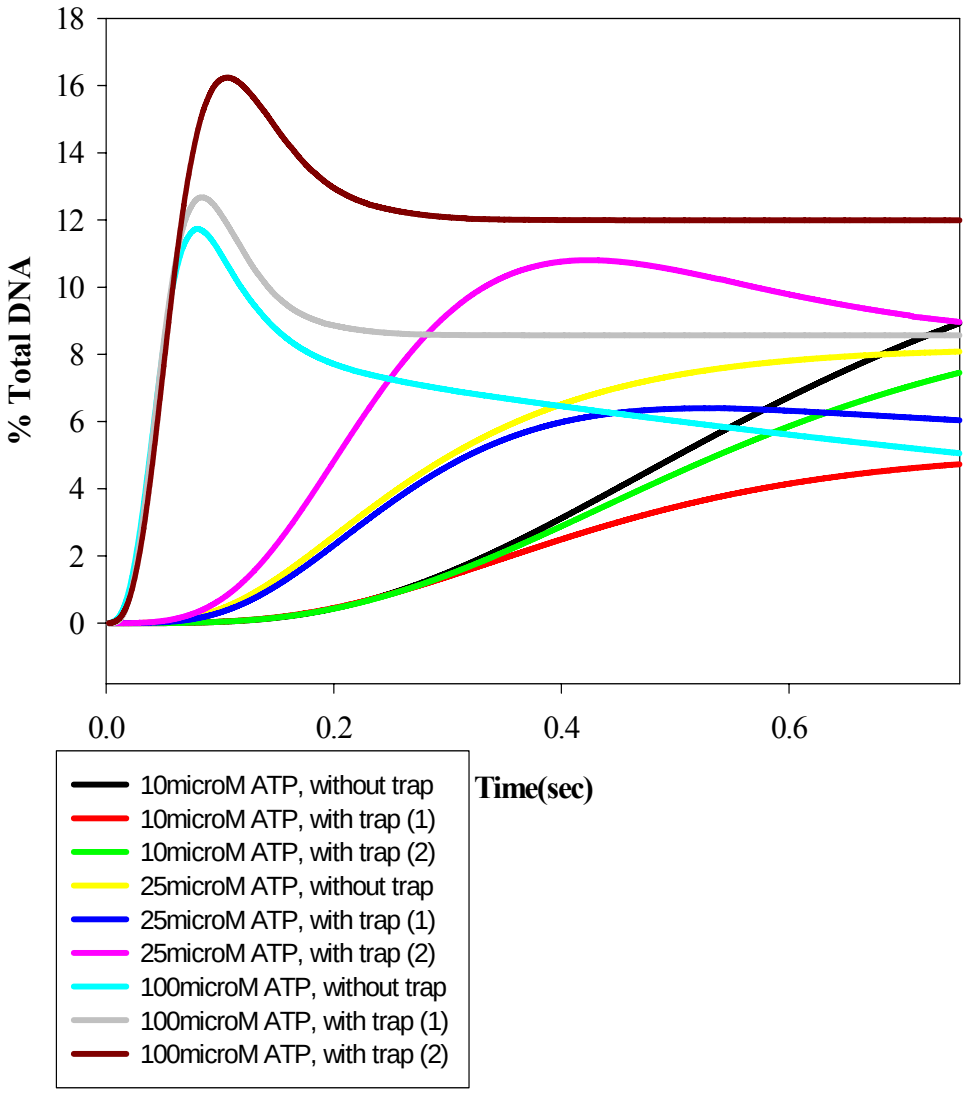

Fig. 30: Simulated time course of the 31 nucleotide intermediate at different ATP concentrations. Graphs were simulated by using the Kinteksim program from Kintek corporation. Three experiments were done at each ATP concentration, one in absence of any trap and two in presence of the trap. (1) and (2) indicate two experiments under the same condition at each ATP concentration.

On comparing the rate constant values in the presence and absence of any trap in each of Tables 6, 7 and 8, we can see that the rate constant values of each nuclease step are more or less the same in the presence or absence of trap. This indicates that the nuclease steps are not affected by the presence of the trap. Also, the rate constant values of the dissociation steps do not seem to vary with the presence or absence of trap. From this, we can say that translocation of the enzyme along the DNA is processive during these steps.

For each DNA-enzyme complex, the rate constant value for the nuclease step is greater than that for the dissociation step. For example, in Table 6, the rate constant values for one dissociation step k_{+7}, for all three reactions (0, 2 and 0.25 s^{-1}), are smaller than the rate constants for the next nuclease step k_{+8} (7.5, 9 and 6 s^{-1}, respectively). This is another way by which the processivity of the enzyme is demonstrated.

For any particular ATP concentration, we took the average of the rate constant values of each cleavage step [ED40→ED38 (k_3), ED38→ED35 (k_4), ED35→ED31 (k_5)] for three reactions at that ATP concentration. Then, we calculated the average of these values for all three cleavage steps. This value, in steps per second, was the calculated value for the rate of translocation of the enzyme along the oligomer, at that particular ATP concentration. Since the enzyme moves in steps of 2-4 nucleotide per step, we considered the average step size of the enzyme to be 3 nucleotide per second. Finally, we multiplied the rate of translocation in steps per second with the step size, to get the rate of translocation in nucleotide per second (see Table 9).

ATP concentration	10μM[a]	25μM[b]	100μM[c]
Average rate constants for the nuclease steps			
k_{+4} (sec^{-1}) (± std. dev.)	8 (± 0)	30 (± 17)	171 (± 9)
k_{+6} (sec^{-1}) (± std. dev.)	6 (± 1)	10 (± 4)	43 (± 6)
k_{+8} (sec^{-1}) (± std. dev.)	7.5 (± 1.5)	6.7 (± 1.2)	60 (± 14)
Average nuclease rate constant (sec^{-1})	7	16	91
Average step size (nucleotides)	3	3	3
Translocation rate (nucleotides / sec)	21	48	273

Table 9: **Calculation of the average translocation rate of the enzyme along the DNA at three different ATP concentrations.** [a] see Table 6; [b] see Table 7; [c] see Table 8;

In one of our experiments we did not pre-incubate RecBCD and DNA before starting the reaction. Rather we put DNA in one syringe, and enzyme mixed with 200μM ATP in the other syringe, and then mixed them to start the reaction (See Fig. 12, Results section). The data that we got from that experiment could not be matched to the graph, simulated by using Mechanisms 2a or 2b. However, when we used Mechanism 3, the simulated graph could be superimposed on the data. In addition, the values of the rate constants were found to be similar to the corresponding values for the reactions done at the same ATP concentration but with the pre-incubation of the enzyme and the DNA. The graph of this experiment is shown in Fig. 31.

In this mechanism there is one additional step including the inactive enzyme-DNA complex E0D40 and two additional rate constants k_{NP+1} and k_{NP-1}. Also the values of k_{+1} and k_{-1} were different from the corresponding values for the reactions with pre-incubation. Values of the rate constants are shown in Table 10.

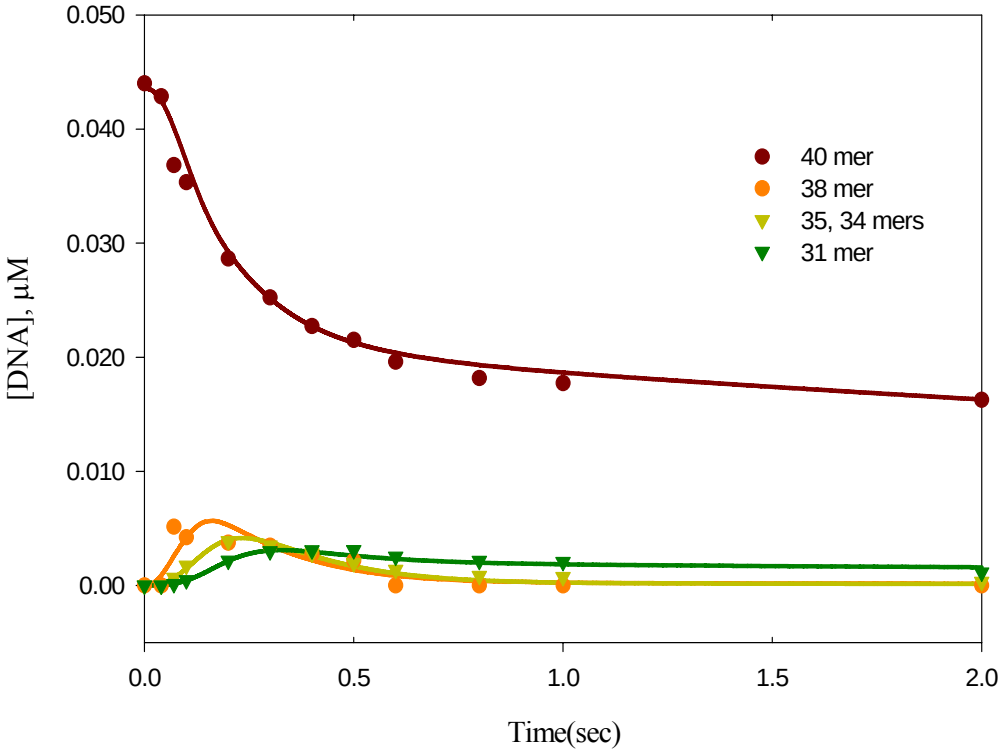

Fig. 31: DNA concentration vs. reaction time plot for the exonuclease reaction at 100µM ATP without the pre-incubation of the enzyme and the DNA. Time courses of the 40mer substrate and the 38mer, 35, 34mers and 31mer intermediates resulting from the nuclease reactions of RecBCD with the oligomer pAG1s at 25ºC, in 25mM Tris-acetate (pH 7.5), 1mM DTT, 100µM ATP and 8mM Mg^{++} (see Fig.21, Results section). This reaction was done without the pre-incubation of the DNA and the enzyme. The enzyme was mixed with ATP and then DNA was added to start the reaction. The graph was simulated by using Mechanism 3.

We carried out an exonuclease reaction with oligomer pAG1rs in the presence of 30μM ATP. The main intermediates of this cleavage reaction were 37, 35, 34, 32, 31, and 29 mers. We used Mechanism 4 to analyze the data obtained from this reaction..

Mechanism 4:

$$\mathbf{E2D40} \xrightarrow{k_{+2'}} \mathbf{E1D40} \xrightarrow{k_{+3'}} \mathbf{ED40} \xrightarrow{k_{+4'}} \mathbf{ED37} \xrightarrow{k_{+6'}} \mathbf{ED35} \xrightarrow{k_{+8'}} \mathbf{ED32} \xrightarrow{k_{+10'}} \mathbf{ED29} \xrightarrow{k_{+12'}} \mathbf{P}$$

$$\mathbf{E + D40} \quad \underset{k_{-1'}}{\overset{k_{+1'}}{\uparrow\downarrow}} \qquad \mathbf{E + D37} \quad \underset{k_{-5'}}{\overset{k_{+5'}}{\uparrow\downarrow}} \qquad \mathbf{E + D35} \quad \underset{k_{-7'}}{\overset{k_{+7'}}{\uparrow\downarrow}} \qquad \mathbf{E + D32} \quad \underset{k_{-9'}}{\overset{k_{+9'}}{\uparrow\downarrow}} \qquad \mathbf{E + D29} \quad \underset{k_{-11'}}{\overset{k_{+11'}}{\uparrow\downarrow}}$$

The values of the 35mer and 34mer were combined and represented as the value of the 35mer in the mechanism. Similarly, we combined the values of the 32mer and 31mer and considered it as the value of the 32mer. Data points were fitted to the above mechanism by simulation. The values of the rate constants are shown in Table 10. It can be noticed that the values of k_1, k_2 and k_3 are similar to those from the nuclease reaction of the oligomer pAG1s at 25μM ATP.

Table 10: Rate constant values from the nuclease reactions done at different conditions with two different oligomers. Rate constant values obtained from the simulations of the nuclease reaction at 100μM ATP by using mechanism 2a, the nuclease reaction at 100μM ATP, with no pre-incubation, by using mechanism 3, the reaction at 500μM ATP by using mechanism 2a, the reaction at 25μM ATP by using mechanism 2a, and the nuclease reaction done with the oligomer pAG1rs at 30μM ATP by using mechanism 4.

Oigomers	pAG1s				pAG1rs	
ATP	100μM	100μM	500μM	25μM	30 μM	
Rate constants	With pre-incubation	No pre-incubation	With trap	No trap	Rate Constants	
$k_{NP+1}(s^{-1})$		0.25				
k_{NP-1} $(\mu M^{-1}s^{-1})$		10				
k_{+1} (s^{-1})	11	0	11	7	$k_{+1'}$ (s^{-1})	11.5
k_{-1} $(\mu M^{-1}s^{-1})$	1	12	0	0	$k_{-1'}$ $(\mu M^{-1}s^{-1})$	2.5
k_{+2} (s^{-1})	23	54	15	4	$k_{+2'}$ (s^{-1})	7
k_{+3} (s^{-1})	160	136	270	35	$k_{+3'}$ (s^{-1})	25
k_{+4} (s^{-1})	166	86	397	50	$k_{+4'}$ (s^{-1})	22
k_{+5} (s^{-1})	0.7	0	4	0.6	$k_{+5'}$ (s^{-1})	2
k_{-5} $(\mu M^{-1}s^{-1})$	0	0	0	0	$k_{-5'}$ $(\mu M^{-1}s^{-1})$	0
k_{+6} (s^{-1})	50	13	84	9	$k_{+6'}$ (s^{-1})	46
k_{+7} (s^{-1})	2	0	2	0.4	$k_{+7'}$ (s^{-1})	0.6
k_{-7} $(\mu M^{-1}s^{-1})$	0	0	0	0	$k_{-7'}$ $(\mu M^{-1}s^{-1})$	0
k_{+8} (s^{-1})	65	15	109	6	$k_{+8'}$ (s^{-1})	12
k_{+9} (s^{-1})	11	2	5	7	$k_{+9'}$ (s^{-1})	1
k_{-9} $(\mu M^{-1}s^{-1})$	3	1	0	0	$k_{-9'}$ $(\mu M^{-1}s^{-1})$	0
k_{+10} (s^{-1})	75	34	192	20	$k_{+10'}$ (s^{-1})	37
					$k_{+11'}$ (s^{-1})	7
					$k_{+12'}$ (s^{-1})	100

We included two extra steps, E2D40 → E1D40, with rate constants k_2, and E1D40→ ED40, with rate constants k_3, before the first cleavage step, ED40 → ED38 (rate constants k_4). The enzyme-DNA complex goes through these three steps after the reaction starts and before the first nuclease product appears. We do not know exactly what happens during these two initial steps. However, the enzyme has to translocate along the DNA a certain distance, so that the 3'end can move from the binding site to the nuclease active site, before the nuclease reaction can take place. We estimated the time of this translocation at three ATP concentrations, using the values of the rate constants of the above three steps. The results are shown in Tables 11, 12 and 13. Also we estimated the distance of this translocation by multiplying the rate of translocation calculated for each ATP concentration with the time period of translocation. The results are, again, shown in Tables 11, 12 and 13.

Relaxation times for 3 initial steps (msec)	10μM ATP No trap	10μM ATP With trap(1)	10μM ATP With trap(2)
$1/k_{+2}$	333	333	200
$1/k_{+3}$	91	83	77
$1/k_{+4}$	125	125	125
Total time (msec)	549	541	402
Average translocation rate (from Table 9) (nt/sec)	21	21	21
Total translocation before 1st nuclease cleavage (Total time X Average translocation rate) / 1000	11.5 nt	11.3 nt	8.4 nt

Table 11: **Translocation of RecBCD before the first nuclease reaction at 10μM ATP.** Total time period and distance (nucleotide) of translocation of RecBCD after the nuclease reaction was started by addition of ATP and before the first cleavage reaction occurred. The enzyme and the DNA were pre-incubated before the reaction and 10μM ATP was added to start the reaction. Two experiments under the same condition at each ATP concentration have been indicated by (1) and (2).

Relaxation times for 3 initial steps (msec)	25μM ATP No trap	25μM ATP With trap(1)	25μM ATP With trap(2)
$1/k_{+2}$	250	167	167
$1/k_{+3}$	29	25	33
$1/k_{+4}$	20	50	50
Total time (msec)	299	242	250
Average translocation rate (from Table 9) (nt/sec)	48	48	48
Total translocation before 1st nuclease cleavage (Total time X Average translocation rate) / 1000	14.3 nt	11.6 nt	12 nt

Table 12: **Translocation of RecBCD before the first nuclease reaction at 25μM ATP.** Total time period and distance (nucleotide) of translocation of RecBCD after the nuclease reaction was started by addition of ATP and before the first cleavage reaction occurred. The enzyme and the DNA were pre-incubated before the reaction and 25μM ATP was added to start the reaction. Two experiments under the same condition at each ATP concentration have been indicated by (1) and (2).

Relaxation times for 3 initial steps (msec)	100μM ATP No trap	100μM ATP No trap	100μM ATP No trap
$1/k_{+2}$	43	42	48
$1/k_{+3}$	6	6	6
$1/k_{+4}$	6	6	5
Total time (msec)	55	54	59
Average translocation rate (from Table 9) (nt/sec)	273	273	273
Total translocation before 1st nuclease cleavage (Total time X Average translocation rate) / 1000	15	14.7	16

Table 13: **Translocation of RecBCD before the first nuclease reaction at 100μM ATP.** Total time period and distance (nucleotide) of translocation of RecBCD after the nuclease reaction was started by addition of ATP and before the first cleavage reaction occurred. The enzyme and the DNA were pre-incubated before the reaction and 100μM ATP was added to start the reaction. Two experiments under the same condition at each ATP concentration have been indicated by (1) and (2).

DISCUSSION:

In this work, we studied the exonuclease reaction of RecBCD. We allowed the enzyme to react with 40 nucleotide long single stranded oligomers. Reactions were allowed to go on for time periods ranging from 0 to 2 secs. We carried out the exonuclease reaction at four different ATP concentrations, 10, 25, 100 and 500 μM. Substrates were radioactively labeled at their 5'-end. After the reaction, we subjected the reaction mixture to sequencing gel electrophoresis, in order to separate the products and the intermediates from the substrate. The gel was dried and was exposed to a storage phosphor screen. The screen was then scanned by a phosphorimager. We could calculate the relative concentrations of the substrates, intermediates and products from the relative intensities of the corresponding DNA bands. The data were analyzed to get the rate constants for the first few steps of the stepwise translocation of the enzyme on the short oligomer.

Exonuclease reaction in the presence or absence of a DNA trap

At each ATP concentration we have two sets of rate constants, one set obtained from reactions done in the presence of an excess of unlabeled DNA trap, and the other without the presence of any trap. A comparison of both show that the reaction rate constants at each step are quite similar in both cases. This indicates that exonucleolytic translocation of the enzyme is processive and the rate of movement is not affected to any considerable amount by the presence the DNA trap. Also at each

step the rate constant for going to the next intermediate by nuclease activity is much larger than the dissociation rate constant. This is another indication of the processivity of the enzyme.

Rate of translocation of the enzyme along the DNA and subsequent nuclease reaction

With decreasing ATP concentrations the values of the rate constants for each step decrease. The unit of the rate constant for going from one step to another is per second. We can get the rate of movement of the enzyme for any step in nucleotide per second by multiplying the value of the rate constant with the number of nucleotides crossed at that particular step. The step size, the number of nucleotides covered in each step remains constant at all ATP concentrations. So decrease of the values of rate constants means the overall rates of movement of the enzyme in each step decrease with decreasing ATP concentrations.

We calculated the average of the rate constants of all the nuclease steps at a particular ATP concentration. From this, we got the translocation rates of the enzyme in three different ATP concentrations, as discussed in the Results section. Our values were close to the unwinding rates found by Lucius et al. (2004a). Table 14 lists the rates obtained in our studies and the ones obtained by Lucius et al. (2004a).

	Unwinding Rate constants	Translocation rate constants
ATP concentrations (μM)	Studies by Lucius et al. (2004) (bp / s)	Present study (from Table 9.) (nt / s)
10	27	21
25		48
37.5	108	
75	225	
100		273
120	343	

Table 14: **Comparison of the unwinding rate constants and translocation rate constants.**

K_m for ATP hydrolysis by RecBCD

Chamberlin and Julin (1996) determined the K_m for ATP hydrolysis by RecBCD, with single stranded oligomers, and it is about 120μM. Roman and Kowalczykowsky (1989a) found that the K_m for ATP in the helicase activity of RecBCD is also 120μM. We chose ATP concentrations (10μM, 25μM, and 100μM) which are lower than these K_m values. We plotted the rate of ATP stimulated translocation of RecBCD on the DNA (obtained from Table 9) against the corresponding ATP concentrations. Fig. 32 shows that the points have formed a straight line, as expected, since the substrate concentrations are less than the K_m.

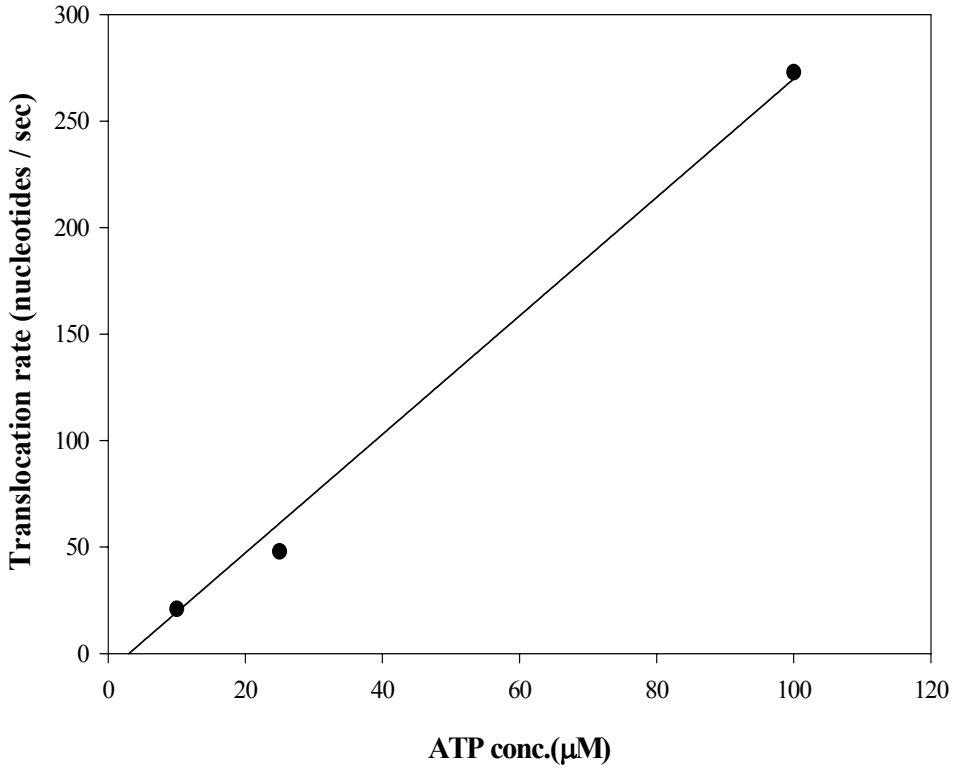

Fig. 32: Plot of translocation rate of RecBCD along DNA vs. ATP concentrations. Data were obtained from Table 9.

Lag time before the first nuclease reaction and the extra steps in the RecBCD-DNA reaction mechanism

We have seen that the lag time for appearances of any intermediate or product increases with decreasing ATP concentration. The presence of this lag time could possibly be explained by considering the structure of the RecBCD-DNA initiation complex. If the enzyme is pre-incubated with the DNA, then it should be bound to the DNA in the form of an initiation complex, at the time of the start of the reaction. As

discussed in the introduction section, the binding site of the enzyme on the 3' end of the DNA is some distance (64 Å, see below) away from the nuclease active site of the enzyme. So, the enzyme has to translocate several bases along the DNA, before the first few bases can reach the nuclease site of the enzyme. The time taken for this translocation could be reflected in the lag time.

Each translocation step includes ATP binding, with or without some conformation change of the enzyme. As the concentration of ATP decreases, it must bind to the enzyme at a slower rate. This could cause the enzyme to move slower and the lag time, during which the 3' DNA end moves from the binding site to the nuclease active site of the enzyme, may become longer.

According to our mechanism, the enzyme goes through the intermediate steps E2D40→E1D40 and E1D40→ED40, and the cleavage step ED40→ED38 before the first cleavage reaction occurs and the first intermediate appears. We calculated the total time during which the enzyme moves through these steps, at 10μM, 25μM and 100μM ATP concentrations. Also, we calculated the translocation rate (in nucleotide per second) of the enzyme at those ATP concentrations. From these we got the number of nucleotides covered by the enzyme during those three initial steps at each ATP concentration (Tables 11, 12 and 13). Our results show that the enzyme can move through 9-15 nucleotides during the steps which cover the lag time period.

The distance between the 3'-end of the DNA and the calcium ion in the nuclease active site was found to be 64Å by using the program Pymol (personal communication, Dr. D. A. Julin.). This distance can also be expressed as 9 – 11 nucleotides depending on the degree of extension of a single DNA strand [assuming

6-7 Å / nucleotide distance between two phosphates, (Saenger, 1983)]. Again, this may be the distance the enzyme must cover after the reaction starts and before the first nuclease reaction occurs, i.e. during the lag time period. This distance is comparable to the one that we got from our calculation (see Tables 11, 12 and 13).

In their mechanism (discussed in the Introduction section), Lucius et al. used two steps with rate constant k_C (Fig. 4). These were different from the regular unwinding steps, with rate constant k_U. The values of k_U increased or decreased with the increase or decrease of the ATP concentration, while the values of k_C were unchanged with the change of the ATP concentrations. In our mechanism also we used two steps E2D40→E1D40 (rate constant k_2) and E1D40→ED40 (rate constant k_3), in addition to the regular cleavage steps and the dissociation steps. But the nature of these steps is different from those used by Lucius et al. We found in our analysis that the rate constant values of both of these steps change with the change of ATP concentration. However, we cannot rule out the possibility that these steps actually are the combinations of more than one step, including one or more ATP independent steps, as shown in the mechanism of Lucius et al.

Experiment without pre-incubation of the enzyme and DNA

We used Mechanism 3 (Fig. 22) for the experiment where the DNA and the enzyme were not pre-incubated, and were mixed with each other to start the reaction. In this scheme, there is a step where DNA and enzyme combine to form an inactive complex (E0D40). This step is absent in the experiment done at the same ATP concentration, but with pre-incubation of the enzyme and the DNA. It can be seen in

Table 10 that the values of the rate constants in all cleavage steps were similar in both the experiments. Ideally, a single mechanism should be applicable for both the reactions. It could be possible that the first dissociation step (rate constant k_1) in scheme 2 is a combination of a dissociation step (E2D40 → E + D40) and a conformation step (E2D40 → E0D40). In this analysis, we could not find a unique ratio of the fraction of the E2D40 complex dissociating, and the fraction of the complex changing conformation. However, the entire analysis was not affected to any considerable extent by the values of these initial steps.

Future studies

This was the first study where the intermediates and products of the exonuclease reaction of RecBCD could be visualized at the pre-steady state level. We studied the rates of appearance, relative amounts, and disappearances of the DNA substrates and products to understand the behavior of the enzyme at different steps of its exonuclease reactions on short oligomers. This ability to see the nuclease intermediates provides us the tools to probe the movement of the enzyme along the DNA oligomers.

This method can also be utilized to learn more about the mechanism of the nuclease reaction of RecBCD. In our study, the oligomer substrate was consistently cleaved at certain positions, and weakly cleaved or not cleaved at all in other positions. The sequence dependence of the nuclease activity can be studied by using oligomers with less random sequences such as a DNA substrate containing a single nucleotide or only two nucleotides arranged in alternative positions.

On studying pre-steady state exonuclease reaction with one of the oligomers (pAG1s), we found one strong band representing a 31 nucleotide intermediate, that appeared during the course of the reaction and then persisted, without disappearing with time. This could be due to some *Chi*-like effect, where strong interaction of the *Chi* site with the RecC subunit causes a strong cut at a position 4-6 nucleotide upstream of the *Chi* site on the 3' end DNA. After this cut, nuclease activity of the enzyme on the 3' end DNA is attenuated. We want to further explore the nucleotide sequence of pAG1s in parts for identifying a *Chi* like sequence having a potential *Chi* like effect.

We also hope to carry out similar studies in the future with double stranded oligomers with or without a *Chi* sequence as substrates. We look forward to contributing more towards understanding RecBCD and other enzymes of similar nature.

REFERENCES:

1. Amundsen, S. K. & Smith, G. R. (2003). Interchangeable parts of the *Escherichia coli* recombination machinery. *Cell* 112, 741-744.
2. Anderson, D. G. & Kowalczykowski, S. C. (1997). The recombination hot spot χ is a regulatory element that switches the polarity of DNA degradation by the RecBCD enzyme. *Genes & Devel* 11, 571-581.
3. Aravind, L., Makarova, K. S. & Koonin, E. V. (2000). Holliday junction resolvases and related nucleases: identification of new families, phyletic distribution and evolutionary trajectories. *Nucleic Acids Res* 28, 3417-3432.
4. Arnold, D. A. & Kowalczykowski, S. C. (2000). Facilitated loading of RecA protein is essential to recombination by RecBCD enzyme. *J Biol Chem* 275, 12261-12265.
5. Arnold, D. A., Handa, N., Kobayashi, I. & Kowalczykowski, S. C. (2000). A novel, 11 nucleotide variant of chi, *Chi**: one of a class of sequences defining the *Escherichia coli* recombination hotspot *Chi*. *J Mol Biol* 300, 469-479.
6. Behme, M. T., Lilley, G. D. & Ebisuzaki, K. (1976). Postinfection control by bacteriophage T4 of *Escherichia coli* recBC nuclease activity. *J Virol* 18, 20-25.
7. Bianco, P. R., Brewer, L. R., Corzett, M., Balhorn, R., Yeh, Y., Kowalczykowski, S. C. & Baskin, R. J. (2001). Processive translocation and

DNA unwinding by individual RecBCD enzyme molecules. *Nature* 409, 374-378.

8. Chen, H.-W., Ruan, B., Yu, M., Wang, J. & Julin, D. A. (1997). The RecD subunit of the RecBCD enzyme from *Escherichia coli* is a single-stranded DNA-dependent ATPase. *J Biol Chem* 272, 10072-10079.
9. Chen, H.-W., Randle, D. E., Gabbidon, M. & Julin, D. A. (1998). Functions of the ATP Hydrolysis Subunits (RecB and RecD) in the Nuclease Reactions Catalyzed by the RecBCD Enzyme from *Escherichia coli. J Mol Biol* 278, 89-104.
10. Cheng, K. C. & Smith, G. R. (1987). Cutting of chi-like sequences by the RecBCD enzyme of *Escherichia coli*. *J Mol Biol* 194, 747-750.
11. Dillingham, M. S., Spies, M. & Kowalczykowski, S. C. (2003). RecBCD enzyme is a bipolar DNA helicase. *Nature* 423, 893-897.
12. Dixon, D. A. & Kowalczykowski, S. C. (1993). The recombination hotspot χ is a regulatory sequence that acts by attenuating the nuclease activity of the *E. coli* RecBCD enzyme. *Cell* 73, 87-96.
13. Dixon, D. A. & Kowalczykowski, S. C. (1995). Role of the *Escherichia coli* recombination hotspot, χ, in RecABCD-dependent homologous pairing. *J Biol Chem* 270, 16360-16370.
14. Eggleston, A. K. & Kowalczykowski, S. C. (1993). Biochemical characterization of a mutant recBCD enzyme, the recB^{2109}CD enzyme, which lacks χ-specific, but not non-specific, nuclease activity. *J Mol Biol* 231, 605-620.

15. Enquist, L. W. & Skalka, A. (1973). Replication of bacteriophage lambda DNA dependent on the function of host and viral genes. I. Interaction of red, gam and rec. *J Mol Biol* 75, 185-212.

16. Finch, P. W., Storey, A., Chapman, K. E., Brown, K., Hickson, I. D. & Emmerson, P. T. (1986). Complete nucleotide sequence of the *Escherichia coli* recB gene. *Nucl Acids Res* 14, 8573-8582.

17. Finch, P. W., Storey, A., Brown, K., Hickson, I. D. & Emmerson, P. T. (1986). Complete nucleotide sequence of *recD,* the structural gene for the alpha subunit of Exonuclease V of *Escherichia coli*. *Nucl Acids Res* 14, 8583-8594.

18. Gabbidon, M. R., Rampersaud, V. E. & Julin, D. A. (1998). Salt-Stable

19. Complexes of the *Escherichia coli* RecBCD Enzyme Bound to Double-Stranded DNA. *Arch Biochem Biophys* 350, 266-272.

20. Goldmark, P. J. & Linn, S. (1972). Purification and properties of the *recBC* DNase of *Escherichia coli* K-12. *J Biol Chem* 247, 1849-1860.

21. Grasby, J. A. & Connolly, B. A. (1992). Stereochemical outcome of the hydrolysis reaction catalyzed by the EcoRV restriction endonuclease. *Biochemistry* 31, 7855-7861.

22. Julin, D. A. & Lehman, I. R. (1987). Photoaffinity labelling of the recBCD enzyme of *Escherichia coli* with 8-azidoadenosine 5'- triphosphate. *J Biol Chem* 262, 9044-9051.

23. Kim, Y. C., Grable, J. C., Love, R., Greene, P. J. & Rosenberg, J. M. (1990). Refinement of Eco RI endonuclease crystal structure: a revised protein chain tracing. *Science* 249, 1307-1309.

24. Kowalczykowski, S. C., Dixon, D. A., Eggleston, A. K., Lauder, S. D. & Rehrauer, W. M. (1994). Biochemistry of homologous recombination in *Escherichia coli*. *Microbiol Rev* 58, 401-465.

25. Kowalczykowski, S. C. (2000). Initiation of genetic recombination and recombination-dependent replication. *Trends Biochem Sci* 25, 156-165.

26. Kuzminov, A., Schabtach, E. & Stahl, F. W. (1994). *Chi* sites in combination with RecA protein increase the survival of linear DNA in Escherichia coli by inactivating exoV activity of RecBCD nuclease. *EMBO J* 13, 2764-2776.

27. Kuzminov, A. (1995). Collapse and repair of replication forks in *Escherichia coli*. *Mol Microbiol* 16, 373-384.

28. Kuzminov, A. (1999). Recombinational repair of DNA damage in *Escherichia coli* and bacteriophage lambda. *Microbiol. Mol Biol Rev* 63, 751-813.

29. Kuzminov, A. & Stahl, F. W. (1999). Double-strand end repair via the RecBC pathway in *Escherichia coli* primes DNA replication. *Genes Dev* 13, 345-356.

30. Lange, C. S. (1975). The repair of DNA double-strand breaks in mammalian cells and the organization of the DNA in their chromosomes. *Basic Life Sci* 5B, 677-683.

31. Lucius, A. L., Vindigni, A., Gregorian, R., Ali, J. A., Taylor, A. F., Smith, G. R. & Lohman, T. M. (2002). DNA unwinding step-size of *E. coli* RecBCD helicase determined from single turnover chemical quenched-flow kinetic studies. *J Mol Biol* 324, 409-428.

32. Lucius, A. L. & Lohman, T. M. (2004a). Effects of temperature and ATP on the kinetic mechanism and kinetic step-size for *E. coli* RecBCD helicase-catalyzed DNA unwinding. *J Mol Biol* 339, 751-771.

33. Lucius, A. L., Jason Wong, C. & Lohman, T. M. (2004b). Fluorescence stopped-flow studies of single turnover kinetics of *E. coli* RecBCD helicase-catalyzed DNA unwinding. *J Mol Biol* 339, 731-750.

34. MacKay, V. & Linn, S. (1976). Selective Inhibition of the DNase Activity of the *recBC* Enzyme by the DNA Binding Protein from *Escherichia coli. J Biol Chem* 251, 3716-3719.

35. Masterson, C., Boehmer, P. E., McDonald, F., Chaudhuri, S., Hickson, I. D. & Emmerson, P. T. (1992). Reconstitution of the activities of the RecBCD holoenzyme of *Escherichia coli* from the purified subunits. *J Biol Chem* 267, 13564-13572.

36. McGlynn, P. & Lloyd, R. G. (2001). Rescue of stalled replication forks by RecG: simultaneous translocation on the leading and lagging strand templates supports an active DNA unwinding model of fork reversal and Holliday junction formation. *Proc Natl Acad Sci U S A* 98, 8227-8234.

37. Muskavitch, K. M. T. & Linn, S. (1981). *recBC*-like Enzymes: Exonuclease V Deoxyribonucleases. In *The Enzymes* (Boyer, P. D., ed.), Vol. 14, pp. 233-250. Academic Press, New York.

38. Myers, R. S. & Stahl, F. W. (1994). *Chi* and the RecBC D enzyme of *Escherichia coli*. *Annu Rev Genet* 28, 49-70.

39. Newman, M., Strzelecka, T., Dorner, L. F., Schildkraut, I. & Aggarwal, A. K. (1994). Structure of restriction endonuclease BamHI and its relationship to EcoRI. *Nature* 368, 660-664.

40. Oliver, D. B. & Goldberg, E. B. (1977). Protection of parental T4 DNA from a restriction exonuclease by the product of gene 2. *J Mol Biol* 116, 877-881.

41. Poteete, A. R., Fenton, A. C. & Murphy, K. C. (1988). Modulation of *Escherichia coli* RecBCD activity by the bacteriophage lambda Gam and P22 Abc functions. *J Bacteriol* 170, 2012-2021.

42. Resnick, M. A. & Martin, P. (1976). The repair of double-strand breaks in the nuclear DNA of Saccharomyces cerevisiae and its genetic control. *Mol Gen Genet* 143, 119-129.

43. Roman, L. J., Eggleston, A. K. & Kowalczykowski, S. C. (1992). Processivity of the DNA helicase activity of *Escherichia coli* recBCD enzyme. *J Biol Chem* 267, 4207-4214.

44. Saenger, W. (1983). *Principles of Nucleic Acid Structure*, Springer-Verlag, New York.

45. Schultz, D. W., Taylor, A. F. & Smith, G. R. (1983). *Escherichia coli* RecBC Pseudorevertants Lacking Chi Recombinational Hotspot Activity. *J Bacteriol* 155, 664-680.

46. Singleton, M. R., Dillingham, M. S., Gaudier, M., Kowalczykowski, S. C. & Wigley, D. B. (2004). Crystal structure of RecBCD enzyme reveals a machine for processing DNA breaks. *Nature* 432, 187-193.

47. Skalka, A. M. (1977). DNA replication--bacteriophage lambda. *Curr Top Microbiol Immunol* 78, 201-237.

48. Smith, G. R. (1990). RecBCD Enzyme. In *Nucleic Acids and Molecular Biology* (Eckstein, F. & Lilley, D. M. J., eds.), Vol. 4, pp. 78-98. Springer-Verlag, Berlin, Heidelberg.

49. West, S. C. (1997). Processing of recombination intermediates by the RuvABC proteins. *Annu Rev Genet* 31, 213-244.

50. Yu, M., Souaya, J. & Julin, D. A. (1998). Identification of the nuclease active site in the multifunctional RecBCD enzyme by creation of a chimeric enzyme. *J Mol Biol* 283, 797-808.